Contents
Previous Section

Minimum Thermal Stability Levels and Controlling Parameters of Methane, As Determined by C_{15}+ Hydrocarbon Thermal Stabilities

By Leigh C. Price

GEOLOGIC CONTROLS OF DEEP NATURAL GAS RESOURCES IN THE UNITED STATES

U.S. GEOLOGICAL SURVEY BULLETIN 2146–K

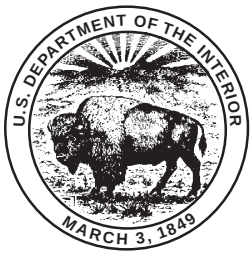

UNITED STATES GOVERNMENT PRINTING OFFICE, WASHINGTON : 1997

CONTENTS

FIGURES

TABLES

Minimum Thermal Stability Levels and Controlling Parameters of Methane, As Determined by C_{15}+ Hydrocarbon Thermal Stabilities

By Leigh C. Price

ABSTRACT

It is taken as law in petroleum geochemistry that C_{15}+ hydrocarbons are thermally destroyed at vitrinite reflectance values of 1.35 percent, that C_2–C_4 hydrocarbons are destroyed at vitrinite reflectance of 2.00 percent, and that rock (greenschist) metamorphism commences at vitrinite reflectance of 4.00 percent. The data of this study lead to the conclusion that these petroleum-geochemical "laws" must be in error. C_{15}+ hydrocarbons, in reality, are thermally stable to vitrinite reflectance values of 7.0–8.0 percent in the natural system, dependent on several variables in deep petroleum basins. C_2–C_4 hydrocarbons are probably thermally stable well into greenschist metamorphic conditions, and methane very probably persists to mantle conditions. The proposed, but erroneous, thermal destruction of C_{15}+ hydrocarbons by vitrinite reflectance levels of 1.35 percent contradicts the extreme bond strengths (82.6–117 kcal/mole) that must be broken for hydrocarbon destruction, bond strengths which require extreme maturation ranks for disruption.

Evidence for significantly greater thermal stability of C_{15}+ hydrocarbons than that portrayed by present-day petroleum-geochemical paradigms is from a large petroleum-geochemical data base that demonstrates that high to moderate concentrations of indigenous C_{15}+ hydrocarbons and bitumen persist in deeply buried rocks at present-day vitrinite reflectance values of 1.35–5.0 percent. Furthermore, moderate to low concentrations of C_{15}+ hydrocarbons and bitumen persist in rocks having vitrinite reflectance values of 5.0–7.0 percent.

Qualitative analyses of (1) bitumen from high-rank rocks (vitrinite reflectance=2.0–7.6 percent), (2) high-rank gases and gas condensates, and (3) bitumen from aqueous-pyrolysis experiments in the hydrocarbon thermal destructive phase all provide significant insight to C_{15}+ hydrocarbon-thermal destruction. Very characteristic carbon-isotopic and chemical assemblages are present, both in hydrocarbon gases and in C_5+ hydrocarbons, in the approach to, and during, C_{15}+ hydrocarbon-thermal destruction.

Part of the reason for the contradiction between actual C_{15}+ hydrocarbon thermal stability and the usually accepted petroleum-geochemical paradigm of C_{15}+ hydrocarbon thermal stability lies in the controlling parameters of organic-matter metamorphism. Organic-matter metamorphism is defined herein as all the reactions involving generation, maturation, and thermal destruction of methane and all C_2+ hydrocarbons (and bitumen), and maturation of kerogen. In present-day petroleum geochemistry theory, organic-matter metamorphism is hypothesized to occur by a parallel series of first-order reactions and thus to be controlled primarily by burial temperature and geologic time. A large body of petroleum-geochemical data strongly suggests, however, that organic-matter metamorphic reactions are not first-order reactions but must be higher ordered reactions. If this is the case, then geologic time plays no, or only a minimal, role in organic-matter metamorphism.

Furthermore, possible generally unrecognized, but important, controlling parameters of organic-matter metamorphism have been suggested by U.S. Geological Survey research. These parameters are (1) the *absence or presence of water in the system*, because C_{15}+ hydrocarbon-thermal destruction is significantly promoted in water-barren systems and is significantly suppressed in water-bearing systems; (2) *increasing fluid pressure*, which strongly suppresses all aspects of organic-matter metamorphism, including C_{15}+ hydrocarbon generation and thermal destruction; (3) product escape from reaction sites, *whether the reaction takes place in an open or closed system* (lack of product escape (closed systems) retards organic-matter metamorphism, and product escape (open systems) promotes organic-matter metamorphism); (4) *increasing temperature*, the principal drive for organic-matter metamorphic reactions, in agreement with present-day petroleum-geochemical paradigms.

INTRODUCTION

The thermal stability of methane in the natural system can be studied in only a few ways. (1) Thermodynamic

calculations can be carried out (Takach and others, 1987; Barker and Takach, 1992). These calculations, however, predict only what should happen, not what will happen, in the natural system because reaction kinetics can, and in this case do, prevent the predictions from thermodynamics from coming to pass. (2) Methane samples can be taken over wide ranges of maturity from sedimentary and low-grade metamorphic rocks. Such samples, by and large, do not exist (have not previously been taken) and would be expensive to collect. Also, the great mobility of methane would render the analytical results from such a sample base ambiguous. (3) High-temperature laboratory experiments can be carried out. It is difficult, however, to relate the conditions of such experiments to equivalent maturity ranks in the natural system. Furthermore, there are no assurances that the experimental parameters would be equivalent to the controlling parameters of the reactions in nature.

Previous research by myself documents the persistence of moderate to high concentrations of C_{15}+ hydrocarbons in rocks at maturation ranks above which methane has been postulated to be thermally stable and moderate to measurable concentrations of C_{15}+ hydrocarbons in rocks at maturation ranks far above the postulated thermal stability limit for methane. Thus, a fourth way exists with which to firmly set the minimum thermal stability limits for methane, determining the maximum thermal stability limits for C_{15}+ hydrocarbons in nature.

As will be discussed, because the observed thermal stability limits for C_{15}+ hydrocarbons are so much greater than the postulated limits for methane, it is insufficient simply to present the data. The reasons for contradictions must be discussed and such a discussion must involve (1) the controlling parameters of hydrocarbon generation and destruction reactions in nature and (2) the origin of the currently accepted paradigms concerning hydrocarbon thermal stability in nature.

Rather than first presenting the data that demonstrates C_{15}+ hydrocarbon thermal stability to extreme maturation ranks, the accepted, and other possible, controlling parameters of hydrocarbon generation and destruction are first discussed. The evidence for highly elevated C_{15}+ hydrocarbon thermal stability is also the evidence that supports controlling parameters of organic-matter metamorphic reactions alternate to those outlined by current petroleum-geochemical paradigms. By this order of presentation, a better subject continuity is achieved.

PARADIGMS OF PETROLEUM GEOCHEMISTRY

According to present-day petroleum geochemistry, organic-matter metamorphic reactions are first-order, and burial temperature and geologic time are the principal controls. As such, it is accepted that geologic time can be substituted for burial temperature in Arrhenius equations describing first-order reactions. Hydrocarbon generation begins at a vitrinite reflectance of 0.5–0.6 percent (fig. 1) and is maximum in intensity by a vitrinite reflectance of 0.9 percent. Organic-matter type can affect these vitrinite reflectance values; however, agreement does not exist among petroleum geochemists on the magnitude or direction of the effect for the different types of organic matter . At vitrinite reflectance of 0.9 percent, C_{15}+ hydrocarbon-thermal destruction commences. By vitrinite reflectance of 1.35 percent all C_{15}+ hydrocarbons have been destroyed. (Some investigators maintain that all C_5+ hydrocarbons are destroyed by this point.) By vitrinite reflectance of 2.0 percent only methane is stable, and by vitrinite reflectance of 4.0 percent methane is destroyed and rock metamorphism begins.

VITRINITE REFLECTANCE (R_o, in percent)	EVENT	
0.5 – 0.9 – 1.35	Oil generation	(Oil deposits)
	Oil destroyed; only $C_1 - C_4$ hydrocarbon gases stable	(Condensate and wet-gas deposits)
2.00	Only methane stable	(Dry gas deposits)
4.00		
4.00+	Rock metamorphism	

Figure 1. Accepted convention regarding occurrence of principal petroleum-geochemical events and hydrocarbon thermal stability.

ALTERNATE HYPOTHESES FOR ORGANIC-MATTER METAMORPHISM

A large published petroleum-geochemical data base does not wholly conform to the above paradigms. Furthermore, interpretation of this data base strongly suggests that alternate petroleum-geochemical models are possible with regards to organic-matter metamorphism.

REACTION ORDER

Increasing burial temperature indeed probably is the principal drive for organic-matter metamorphic reactions; however, organic-matter metamorphic experiments carried out in closed, pressurized, water-wet systems that are thought to simulate nature are not first-order reactions but are higher ordered reactions (Rogers and others, 1962; Bostick, 1970; Brooks, 1971; McIntyre, 1972; Hesp and

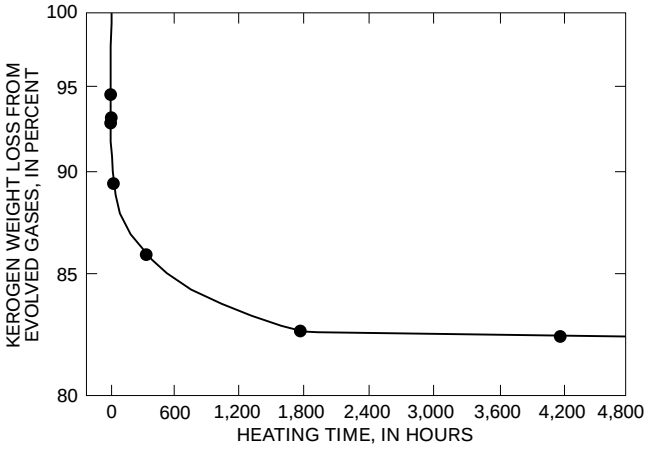

Figure 2. Reaction extent versus time for aqueous-pyrolysis experiments on shale of the Middle Pennsylvanian Anna Shale Member (total organic carbon=29.6 percent, type II/III organic matter). Short-time experiments were 4, 12, 24, and 48 hours. Evolved gases include carbon dioxide, methane, ethane, propane, n-butane, and i-butane.

Rigby, 1973; Goodarzi and Murchison, 1977; Ishwatari and others, 1977; Chung and Sackett, 1978; Pearson, 1981; Price, 1983, 1985) (fig. 2). It must be stressed that first-order reactions plot as straight lines on plots such as figure 2, whereas higher ordered reactions do not. The experiments referenced directly above lead to the conclusion that the effect of geologic time on organic-matter metamorphism may be overestimated, and ample geologic evidence supports this possibility (Price, 1983; Quigley and MacKenzie, 1988; Barker, 1991). As discussed in Price (1983), the original evidence (Karweil, 1956; Lopatin, 1971; Connan, 1974) for the hypothesis of geologic time being a controlling parameter in organic-matter metamorphism was obtained from geologically older sedimentary basins. In these basins, rocks at high maturation rank are at low present-day burial temperatures. Thus, it was concluded that the same extent of organic-matter metamorphism would take place over long geologic times at low burial temperatures as would take place in short geologic times at higher burial temperatures. As discussed in Price (1983), however, in *all* the basins studied by Karweil, Lopatin, and Connan, there is compelling geologic evidence, apparently not originally observed, that suggests high to extreme paleo-heat flow existed in these basins, heat flows that later decayed to the low, present-day values. Thus, the original data base for the hypothesis of geologic time as a controlling parameter in organic-matter metamorphism was flawed. Instead, the principal influence geologic time has on organic-matter metamorphic reactions is simply that the longer rocks exist in sedimentary basins, the better chance they have to be affected by high heat flows from different geologic processes.

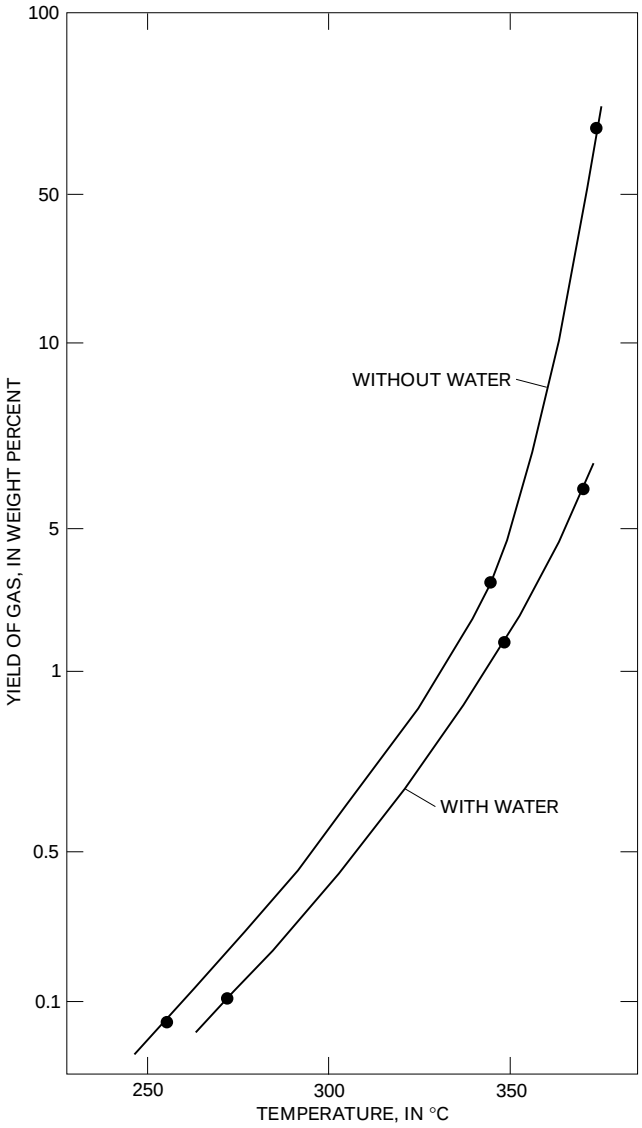

Figure 3. Effect of water on thermal cracking to gas of a middle oil distillate fraction from the Kingfish oil field, Gippsland Basin, at different experimental temperatures. Modified from Hesp and Rigby (1973).

EFFECT OF WATER

Hesp and Rigby (1973) demonstrated that water significantly retards the thermal destruction of hydrocarbons (fig. 3), and M.D. Lewan (written commun., 1993) documented the same effect in his hydrous-pyrolysis experiments. Aqueous-pyrolysis experiments of Wenger and Price (1991) and Price and Wenger (1991) and aqueous crude-oil solubility measurements of Price (1981) also support this conclusion. Hoering and Ableson (1964) reacted kerogen with D_2O at 100˚C for 7 days, dried the kerogen, and then heated it under vacuum at 200˚C and found that the hydrocarbons cracked from the kerogen were deuterated. They thus demonstrated

that, during mild catagenesis, kerogen exchanges, and perhaps incorporates, water into its structure. This phenomenon has also been observed (Price and Wenger, 1991; Wenger and Price, 1991) in aqueous-pyrolysis experiments on six rocks containing different types of organic matter. In the lower temperature (pre-hydrocarbon-generation) experiments, Rock-Eval hydrogen index significantly increased relative to the values for the unreacted rocks. Furthermore, the same phenomenon is evident in natural samples. The significant increase in hydrogen index for the coals of figure 4 in the range from vitrinite reflectance of 0.3 percent to vitrinite reflectance of 0.7 percent, a trend also present in Bertrand's (1984) coal set (fig. 5), previously was attributed to loss of volatiles, especially carbon dioxide, with increasing rank. Aqueous-pyrolysis experiments carried out on a hydrogen-poor lignite (Price, 1989a, figs. 7–10; Wenger and Price, 1991) demonstrate the copious amounts of CO_2 that coals generate at low maturation ranks (fig. 6), even before intense C_{15}+ hydrocarbon generation begins (fig. 7). Such a loss of carbon dioxide would increase coal (and kerogen) hydrogen content and thus Rock-Eval hydrogen index. For example, in the above-mentioned aqueous-pyrolysis experiments with lignite, hydrogen index increases from 55 in the original unreacted sample to maximal values of 78–84 at experimental temperatures of 175˚C–250˚C. Mass-balance calculations for these experiments suggest, however, that carbon dioxide loss alone cannot account for the increase in hydrogen index. The shortfall most likely is made up by incorporation of water into the lignite. This would also increase the hydrogen content, and thus the hydrogen index of the lignite, confirming the earlier results of Hoering and Abelson (1964). Given this proposed interaction of water with lignite, excess oxygen should be present in the system from incorporation of the oxygen from water into the kerogen. Such is the case because the lignite at higher aqueous-pyrolysis temperatures generates more than five times more CO_2 than possible (fig. 6) given the original Rock-Eval oxygen index (72) of the lignite.

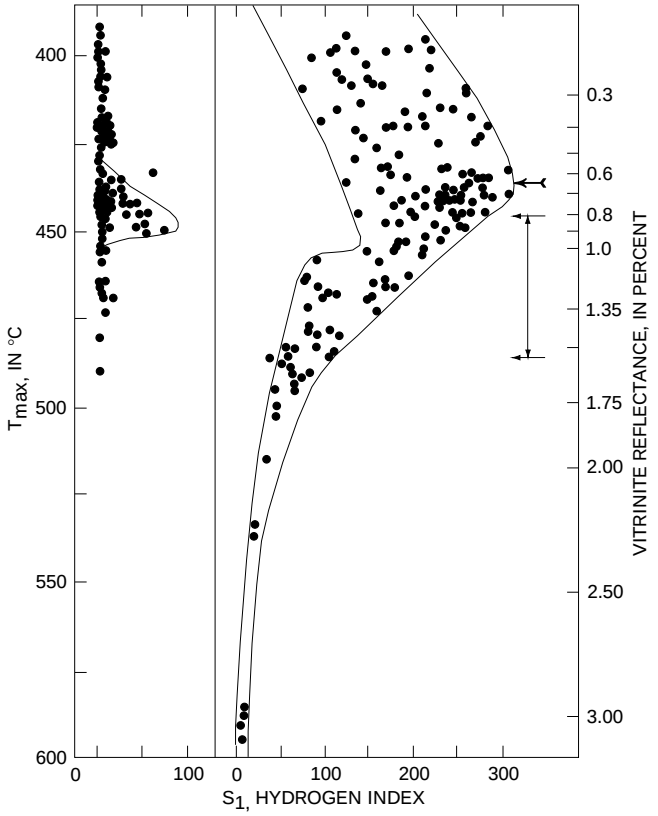

Figure 4. T_{max} and vitrinite reflectance (R_o) versus S_1 (in milligrams of hydrocarbon per gram of rock) and S_2 (hydrogen index) pyrolysis peaks (normalized to organic carbon [OC]) for Paleozoic to Tertiary coals worldwide. The feathered arrow indicates the maximum in the hydrogen index data. The bracketed vertical arrows indicate the maximum loss in the hydrogen index. Data from Teichmüller and Durand (1983), whose original vitrinite reflectance data was given in R_m values; R_m was converted to R_o by R_m=1.066 R_o.

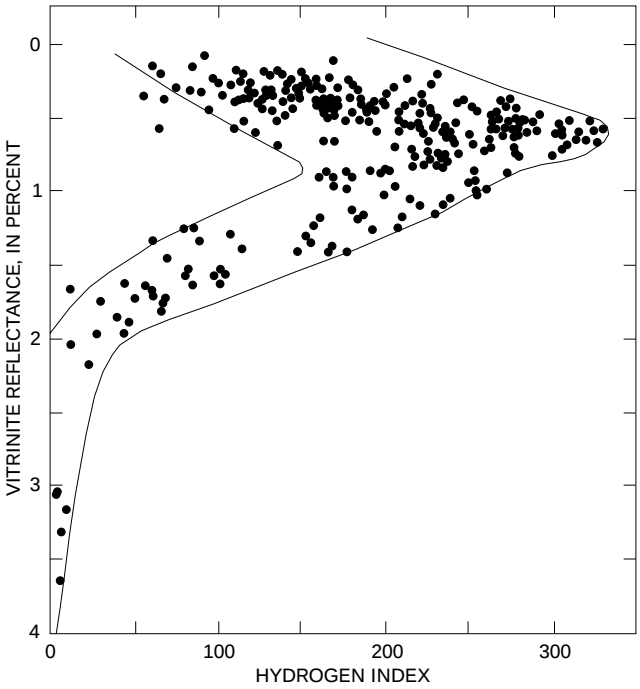

Figure 5. Mean vitrinite reflectance (R_m) versus hydrogen index (S_2 pyrolysis peak) for coals worldwide and all geologic ages. Modified from Bertrand (1984).

SYSTEM OPENNESS

By Le Chatelier's principle (Sienko and Plane, 1961), lack of reaction-product removal during a chemical reaction, in reversible reactions, can create a stress on a system, a stress that can impede or halt the reaction. This possibility especially applies to systems in which the reactants are liquid

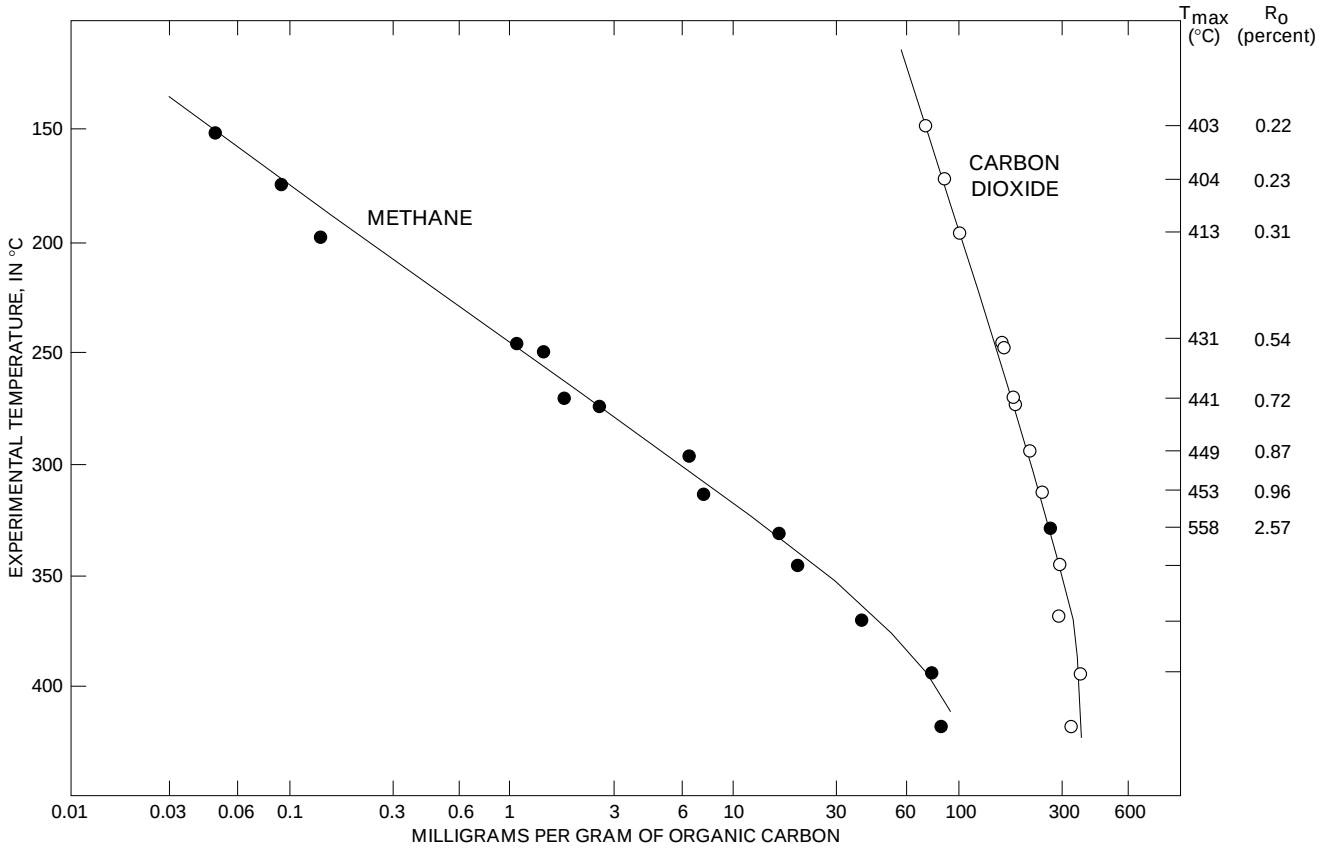

Figure 6. Amounts of carbon dioxide and methane generated by aqueous pyrolysis of the Paleocene Rattlesnake Butte lignite of the Fort Union Formation versus experimental temperature, measured Rock-Eval T_{max}, and estimated vitrinite reflectance (R_o).

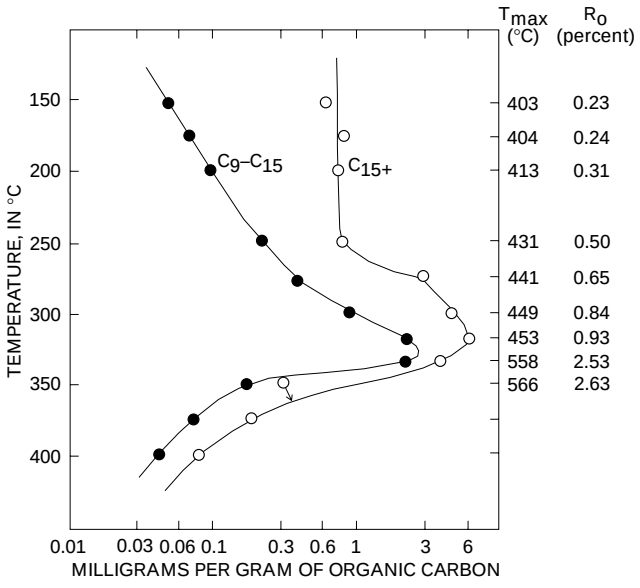

Figure 7. Amounts of C_9–C_{15} and C_{15}+ saturated hydrocarbons generated by aqueous pyrolysis of the Paleocene Rattlesnake Butte lignite of the Fort Union Formation versus experimental temperature, measured Rock-Eval T_{max}, and estimated vitrinite reflectance (R_o).

or solid and one or more of the products is gas, as is the case in both hydrocarbon-generation and hydrocarbon-thermal destruction reactions. Clearly, organic-matter metamorphic reactions are not reversible reactions for the most part. It is possible, however, but has not been demonstrated, that intermediate species in hydrocarbon-thermal destruction reactions may exist in reversible or equilibrium situations. If such is the case, then one might expect Le Chatelier's principle to apply to these reactions in closed-chemical systems, and experimental results (discussed later) suggest that this may be the case. Previously, petroleum geochemists (including this author) have considered primary petroleum migration from organic-rich rocks to be very efficient, mostly removing hydrocarbons from their generation sites (Price and others, 1984; Cooles and others, 1986; Leythaueser and others, 1987, 1988; MacKenzie and others, 1987; Talukdar and others, 1987; Ungerer and others, 1987; Espitalié, Maxwell, and others, 1988). Efficient primary migration implies an open-chemical system; however, other considerations (Price and LeFever, 1992; Price, 1994) suggest that in reality most generated hydrocarbons (1) remain locked in source rocks, (2) generally escape only when such rocks are disrupted by faulting, and (3) are lost to drilling muds during the

rock trip up the wellbore in drilling operations (discussed following and in Price and LeFever, 1992) and thus are not measured in the laboratory. By these considerations, hydrocarbon-generation and thermal-destruction reactions could often take place in closed chemical systems with little or no meaningful product escape. Experiments, discussed following, demonstrate that hydrocarbon-destruction reactions are impeded or halted in closed chemical systems. Thus, in my opinion, the openness of organic-matter metamorphic reaction sites in nature may be a pivotal, and generally unrecognized, controlling parameter in organic-matter metamorphism.

It must be stressed that regional shearing of fine-grained rocks opens up closed chemical systems, and relieves high fluid pressures and thus strongly promotes both organic-matter and inorganic (rock) metamorphism at much lower burial temperatures than would be the case in unsheared rocks. Results of Goffé and Villey (1984) corroborate this point.

FLUID PRESSURE

Some investigators believe that fluid pressure plays no role in organic-matter metamorphism (Hunt, 1979), plays a role subordinate to temperature (Tissot and Welte, 1984), or promotes hydrocarbon-thermal destruction (Braun and Burnham, 1990). Data from the laboratory and (or) nature demonstrate that increasing fluid pressure retards many aspects of organic-matter metamorphism, including hydrocarbon-thermal destruction (Hesp and Rigby, 1973; McTavish, 1978; Cecil and others, 1979; Goffé and Villey, 1984; Connan and others, 1991; Dominé, 1991; Price and Wenger, 1991; Dominé and Enguehard, 1992). Contrasting experimental results of Monthioux and others (1986), who found that pressure has no effect on organic-matter metamorphism, were attributed to experimental technique by Price and Wenger (1991). Monthioux and others (1986) carried out their experiments in small gold bags that became totally flattened, containing no dead volume, during the experiments. Such a lack of dead volume precludes product escape from reaction sites. Such lack of product escape could so strongly retard organic-matter metamorphism that the effects of pressure would not be observed. Larger pressure vessels, which have dead volumes for product removal from the reaction sites, give different experimental results.

A series of aqueous-pyrolysis experiments (Wenger and Price, 1991) was performed on a variety of organic-rich rocks (table 1) under a wide range of conditions; among these experiments were experiments on the Retort Phosphatic Shale Member of the Lower Permian Phosphoria Formation (type II–S organic matter) at three different constant temperatures as a function of increasing static-fluid pressure. The degree to which these laboratory experiments replicate natural organic-matter metamorphism was addressed by comparing the compositions of aqueous-pyrolysis bitumens from the different experiments with those of natural products—crude oils, gas-condensates, and rock extracts—at equivalent maturities. Close correlations were found, and the lack of any detectable laboratory artifacts (compounds not found in abundance in natural samples) in the aqueous-pyrolysis bitumens suggests that these experiments had closely replicated nature.

Variable-temperature and constant-pressure experiments also were performed on the Phosphoria shale. Qualitative analyses of the products from these constant-pressure, variable-temperature experiments (immature to post-supermature maturation ranks) delineate changes in both the generation products and reacted rocks due to increasing maturation rank (increasing experimental temperature). By comparing results of these analyses with results of the same analyses for the constant-temperature, variable-pressure experiments, it is evident that increasing static-fluid pressure strongly retarded hydrocarbon generation, maturation, and thermal destruction. For example, at 287˚C and 31 bars pressure the Phosphoria shale is in the middle of main-stage hydrocarbon generation (fig. 8). When system pressure was increased to 965 bars at 287˚C, hydrocarbon generation was suppressed (fig. 9), and the extent of the quantitative reaction became equivalent to that of the threshold of intense hydrocarbon generation at an experimental temperature of 225˚C (fig. 8). Concurrently, the hydrogen index of the reacted and Soxhlet-extracted rock also greatly increased, from 209 at 287˚C and 31 bars to 371 at 287˚C and 965 bars, as the amount of generated products decreased due to the pressure increase. Likewise, qualitative aspects of the extracted bitumen shifted from moderately mature to immature values. Thus, at 287˚C and 31 bars gas chromatograms (not shown)

Table 1. Samples on which aqueous-pyrolysis experiments were carried out.

Rock	Total organic carbon content (weight percent)	Hydrogen index	Type of organic matter
Pennsylvanian Anna Shale Member	25	320	II/III
Devonian-Mississippian Bakken Formation	14	570	II
Eocene Green River Formation	14	805	I
Paleocene Rattlesnake Butte lignite in Fort Union Formation	50	70	IV/III
Permian Phosphoria Formation	22	620	II-S
Los Angeles Basin mid-Miocene shale	5	500	II

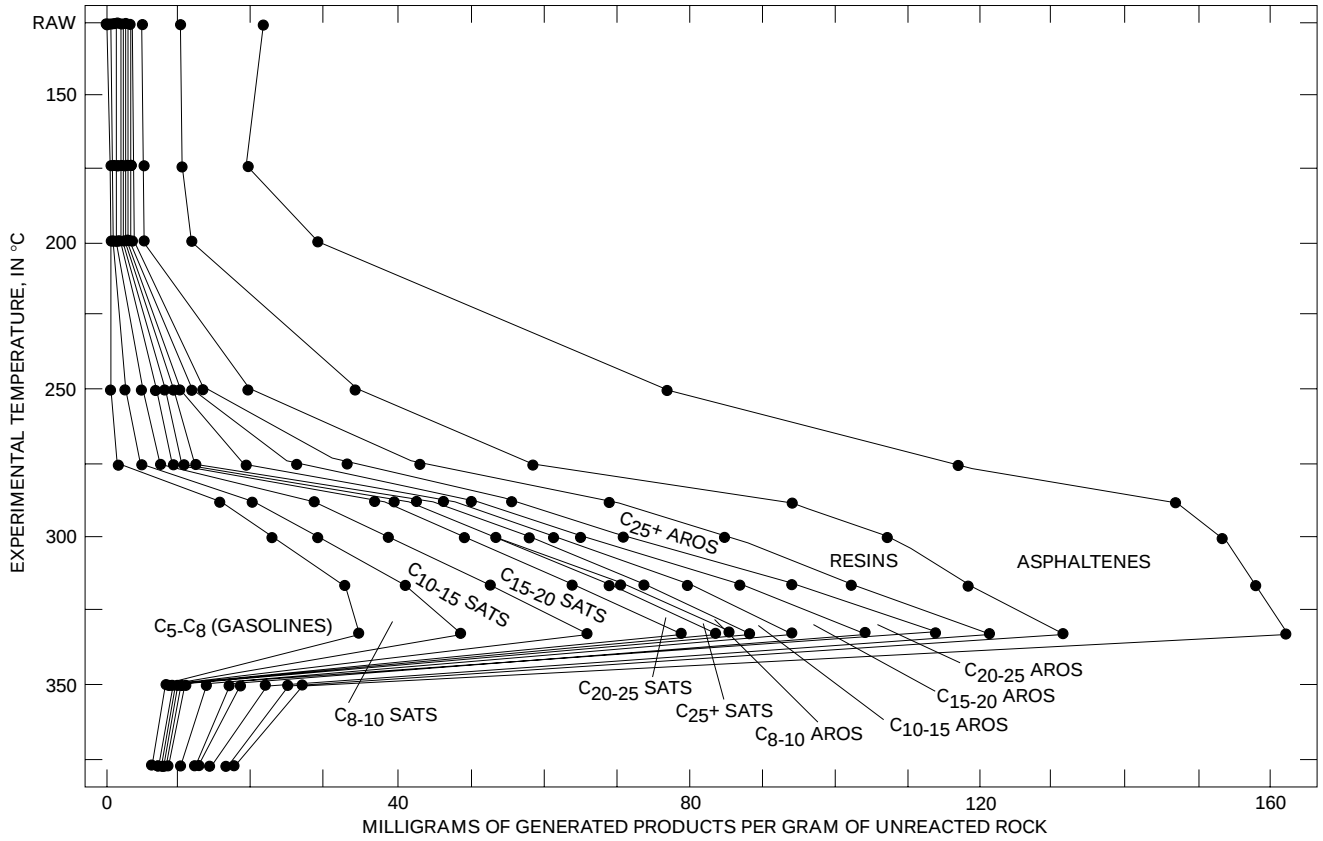

Figure 8. Concentration of various products generated by aqueous pyrolysis of shale from the Lower Permian Phosphoria Formation as a function of increasing experimental temperature. "RAW," original unaltered rocks; SATS, saturated hydrocarbons; AROS, aromatic hydrocarbons.

of the C_8+ saturated hydrocarbons had moderately mature characteristics: (1) n-paraffin concentrations generally greater than those of both adjacent isoprenoid hydrocarbons and of biomarker peaks and (2) a regular n-paraffin profile (Price and Wenger, 1991, fig. 7). However, at 287˚C and higher pressures C_8+ saturated-hydrocarbon distributions become increasingly immature; the 287˚C, 865-bar sample was quite immature (n-paraffin concentrations equal to or less than those of adjacent isoprenoid hydrocarbons and biomarker peaks, an irregular n-paraffin profile, and a bimodal distribution in the naphthene envelope). These and much other data (Price and Wenger, 1991) demonstrate that increasing static-fluid pressure retards hydrocarbon generation.

With increasing temperature, by 350˚C and 118 bars, the aqueous-pyrolysis experimental system for the Phosphoria shale was strongly into the thermal cracking phase for C_5+ generation products, as indicated by a decrease in the sum of the C_5+ products from a maximum value (versus temperature) of more than 160 mg/g of rock at 333˚C to 31 mg/g rock at 350˚C (fig. 8). With increasing pressure, however, by 1,077 bars and 350˚C, thermal cracking was retarded such that the sum of the C_5+ products increased from 31 to 88 mg/g rock (fig. 10). Furthermore, although the C_1–C_4 hydrocarbon gases made up 58.0 percent normalized percent of all the products by weight at 350˚C and 118 bars, these gases made up only 16.9 percent of the total product by weight at 350˚C and 1,077 bars. At 350˚C with increasing pressures, qualitative aspects (maturation indices) of the bitumen and reacted rock also took on less mature characteristics and (or) values, as was true in the 287˚C experiments. Thus, data from the 350˚C experiments demonstrate that increasing static-fluid pressure also strongly retards the thermal destruction of C_{15}+ hydrocarbons at a given temperature.

Results of these experiments have implications regarding both hydrocarbon generation and thermal destruction in nature. Consider two geologic situations, one in which the geothermal gradient is high and the other in which it is low, and all other things equal. Hydrocarbon generation may be expected to occur at lower burial temperatures in the high geothermal gradient case as compared to the low geothermal gradient case due to shallower burial depths and thus lower static-fluid pressures. The retardation of C_{15}+ hydrocarbon-thermal destruction at high static-fluid pressures helps explain the presence of moderate to high C_{15}+ hydrocarbon concentrations in deep (7–10 km) high-rank rocks of deep

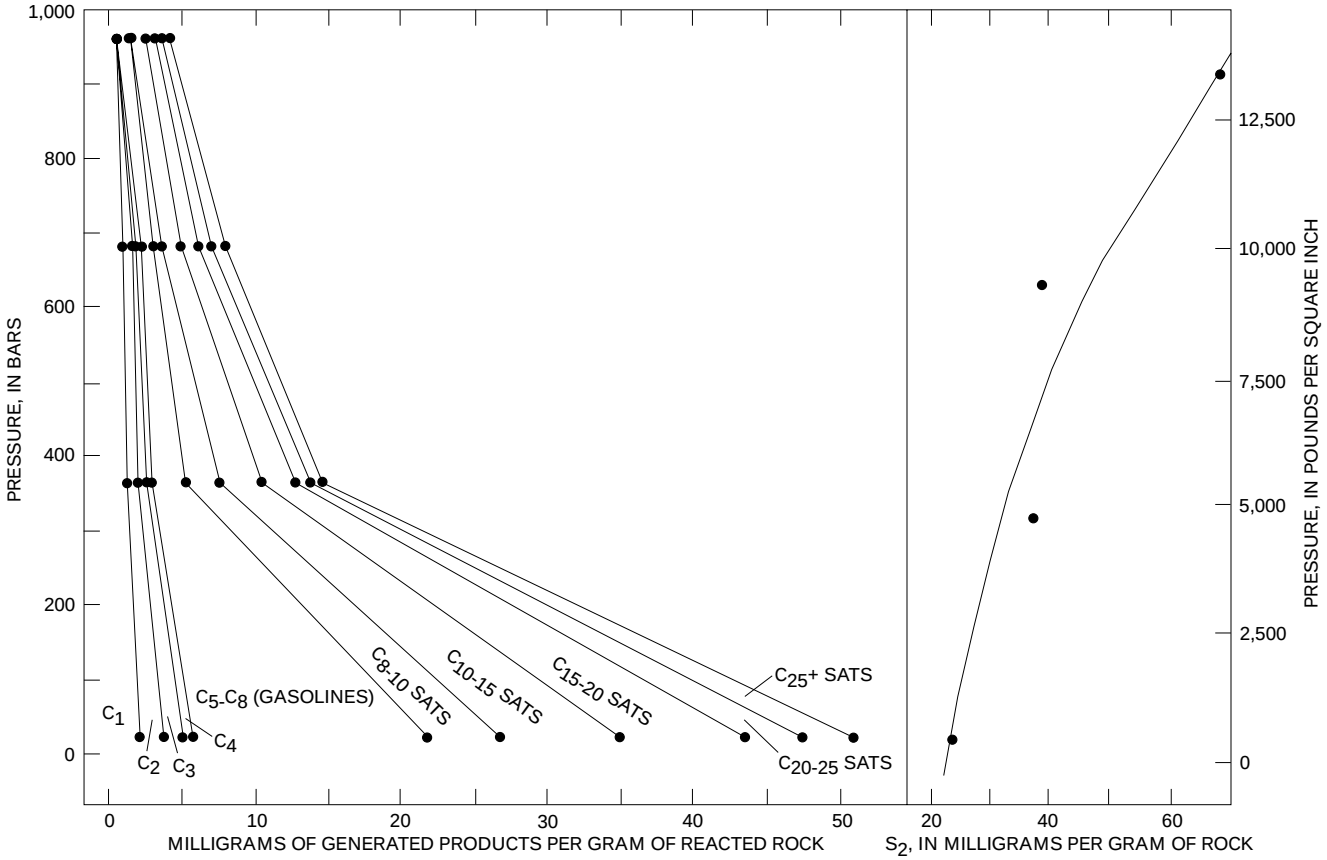

Figure 9. Concentration of various products and S_2 Rock-Eval pyrolysis peak of Soxhlet-extracted reacted rock plotted versus increasing system static fluid pressure at a reaction temperature of 287˚C. SATS, saturated hydrocarbons.

wellbores in which such hydrocarbons would not otherwise be expected (discussed following).

Abnormal fluid pressures would accompany maximum heat flow in deep basins. Thus, with increasing burial, the tendency of higher burial temperatures to destroy C_{15}+ hydrocarbons would be offset by concurrent increasing static-fluid pressures, which inhibit C_{15}+ hydrocarbon-thermal destruction. Light oil, condensate, and, especially, gas deposits may be expected at burial temperatures higher than predicted by some organic-geochemical models because of the suppression of C_{15}+ hydrocarbon-thermal destruction by high static-fluid pressures. Computer modeling of hydrocarbon generation and maturation does not employ static-fluid pressure as a variable, and inclusion of this controlling parameter of organic metamorphism in such models may allow nature to be more closely represented.

ORGANIC-MATTER TYPE

Organic-matter type, in my opinion, plays a dominant and generally unappreciated role in hydrocarbon generation and, to a lesser extent, in the generation of high-rank methane. Different types of organic matter have different distributions of bond strengths, and thus different activation energies, and as such require significantly different burial temperatures for hydrocarbon generation. Although it is recognized that some differences exist in the reactivities of different types of organic matter, in my opinion, the magnitude of these differences is unappreciated. Also, petroleum geochemists do not agree as to the direction of the effect for any given organic-matter type.

Type II–S (sulfur-rich, marine) organic matter has weak, sulfur-bearing bonds and begins hydrocarbon generation first, at low (vitrinite reflectance 0.4 percent?), but yet undefined, maturation ranks, yielding a very heavy, sulfur-rich oil (Lewan, 1985; Orr, 1986; Wenger and Price, 1991). Type II–S organic matter retains significant hydrocarbon-generation potential to high ranks, and oil quality dramatically improves with rank. Type III organic matter has oxygen-bearing bonds, some of which are relatively weak; it begins hydrocarbon generation next at vitrinite reflectance of 0.6 percent and loses all hydrocarbon-generation potential by vitrinite reflectance of 2.00 percent (figs. 4, 5, 14, 18). Types I and II organic matter have relatively strong bonds and generate hydrocarbons last; the higher the original hydrogen content of their kerogen, the higher the burial

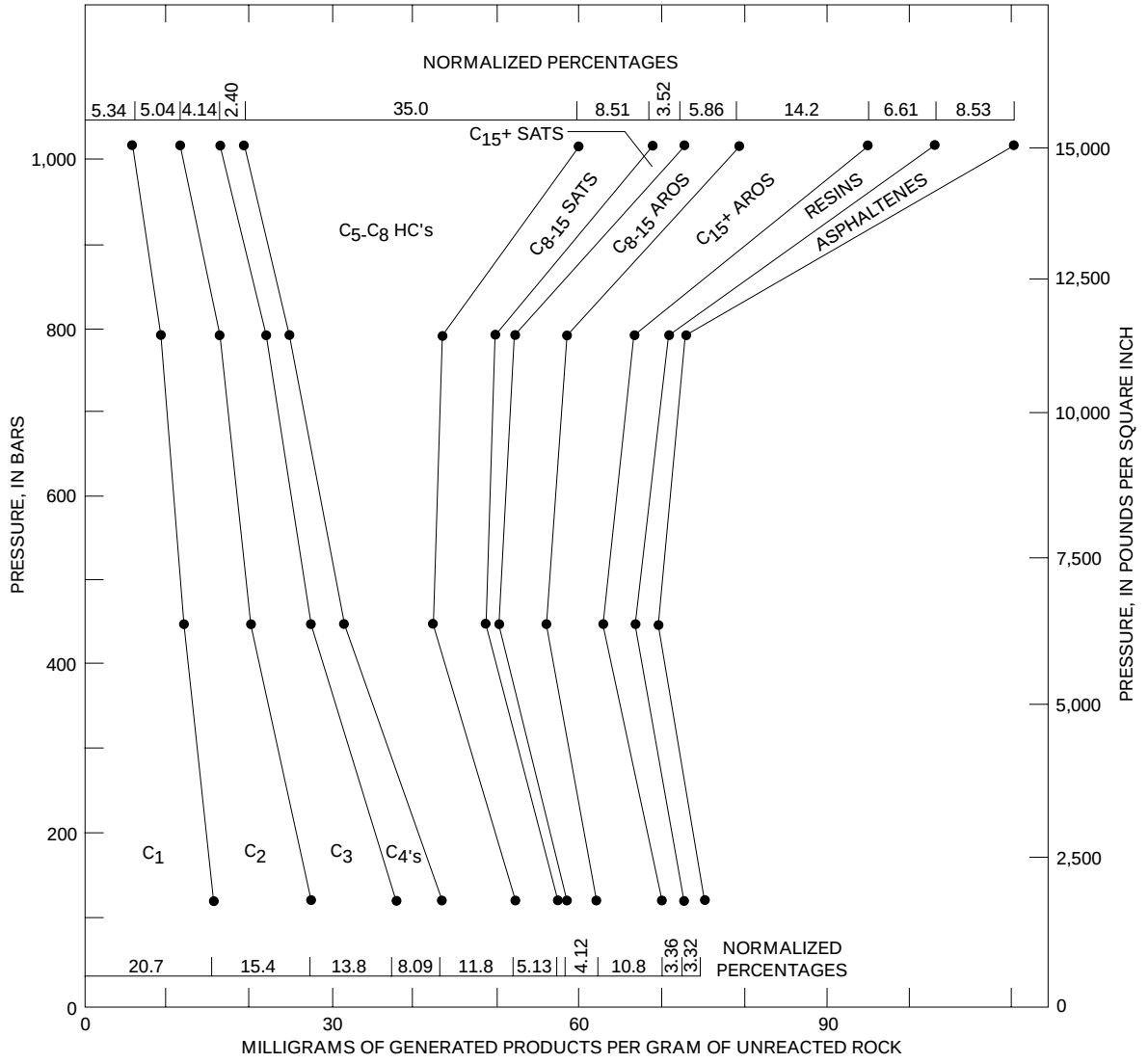

Figure 10. Concentration of various products generated by aqueous pyrolysis of shale from the Lower Permian Phosphoria Formation at 350˚C as a function of increasing static fluid pressure. Normalized percentages which each component or compound group make up of the total product are shown for the 350˚C, 118-bar and 350˚C, 1,077-bar experiments. C_1 to C_4's are the hydrocarbon gases methane through the butanes; SATS are saturated hydrocarbons; AROS are aromatic hydrocarbons.

temperature needed to initiate hydrocarbon generation (Price, 1988, 1991). This last conclusion contrasts with models presented by some investigators (see Tissot and others, 1987, fig. 26, for example), wherein type II organic matter is held to begin hydrocarbon generation before type III organic matter. Ungerer (1990) also has proposed that type II organic matter generates before type I organic matter, which generates before type III organic matter. These hydrocarbon-generation models are derived from Rock-Eval kinetics, in which thermal kerogen degradation occurs in open, low-pressure, water-free systems, and significant percentages of reaction products are chemical artifacts not found in nature. In contrast, natural hydrocarbon generation occurs in high-pressure, water-bearing, closed systems. Rock-Eval is a convenient method with which to examine kerogen thermal degradation; however, it is tenuous to extrapolate to nature results from experiments carried out under conditions unlike those in nature, where some products from those experiments are unlike hydrocarbon-generation products in nature.

Hydrous-pyrolysis (Lewan, 1983, 1985, 1993) and aqueous-pyrolysis (Price and Wenger, 1991; Wenger and Price, 1991) experiments carried out in closed, water-bearing, pressurized systems yield products that are very similar, and commonly identical, to those in nature, and thus these experimental techniques clearly simulate natural organic-matter metamorphism much better than does Rock-Eval pyrolysis. Results from such experiments yield a

significantly different scheme of reaction kinetics for the different types of organic matter than does Rock-Eval pyrolysis.

In the aqueous-pyrolysis experiments of Wenger and Price (1991) and Price and Wenger (1991), six rocks (table 1) of widely different organic-matter types were run under the same experimental conditions (150˚–450˚C reaction temperatures, in 25˚C intervals, at constant pressures, for 30 days; see Price and Wenger [1991] for a description of experimental conditions and techniques). Because all experimental conditions were held constant except for organic-matter type, the reaction extent of the different organic-matter types (and thus organic-matter type reactivity) can be directly compared at each experimental temperature (fig. 11). In figure 11, C_8+ saturated-hydrocarbon gas chromatograms for the starting rock ("Raw Rock") and two experimental temperatures are presented for three of the rocks of table 1. Comparison of the gas chromatogram of the 200˚C experiment with that of the raw (starting) sample for the carbonaceous shale from the Anna Shale Member of the Middle Pennsylvanian Pawnee Limestone (moderately hydrogen poor type III/II organic matter, hydrogen index 320) shows distinct differences between the two chromatograms. In the 200˚C Anna chromatogram (1) there are noticeably greater concentrations of n-paraffins; (2) ratios of different compounds to each other have changed (for example, n-C_{18}/phytane [an especially useful maturity index that can be used to track hydrocarbon generation], n-C_{17}/pristane, and n-C_{16}/i-C_{18}); and (3) there are noticeable differences in the peak distribution of the biomarker range compounds (n-C_{26} to n-C_{35}). The chromatogram for the 275˚C Anna Shale experiment shows extreme differences as compared to that of the raw sample because by 275˚C this rock is well into intense hydrocarbon generation.

In contrast, C_8+ saturated-hydrocarbon gas chromatograms for the raw and 200˚C sample of the mid-Miocene shale from the Los Angeles Basin (moderately hydrogen rich, type II organic matter, hydrogen index 500) demonstrate only minor differences from one another because only insignificant hydrocarbon generation has taken place at 200˚C. Although noticeable hydrocarbon generation has occurred in this rock by 275˚C, the 275˚C Los Angeles sample still exhibits pronounced immature characteristics compared to the 275˚C Anna sample: (1) an irregular n-paraffin distribution; (2) lower ratios of n-C_{17} and n-C_{18} relative to their adjacent isoprenoid hydrocarbons pristane and phytane; (3) a bimodal naphthenic envelope (especially noticeable in the C_{15}+ saturated-hydrocarbon gas chromatogram, not shown); (4) noticeable biomarker peaks; and (5) a lower concentration of C_{14} hydrocarbons.

C_8+ saturated-hydrocarbon gas chromatograms for the raw and 200˚C shale samples from the Eocene Green River Formation are identical because no hydrocarbon generation has occurred in the very hydrogen rich organic matter (type I, hydrogen index 805) of this rock at 200˚C. Furthermore, the reaction extent in the organic matter of the Green River Shale is minimal at 275˚C as compared to that of the other two rocks at 275˚C. The data of figure 11 clearly demonstrate that significantly greater burial temperatures are required to initiate main-stage hydrocarbon generation in hydrogen-rich organic matter than in hydrogen-poor organic matter. These differences are probably caused by higher activation energies in hydrogen-rich organic matter as compared to hydrogen-poor organic matter. In sulfur-poor hydrogen-rich organic matter, activation energies are believed to increase with increase in the original hydrogen content of the kerogen.

The control that organic-matter type has on kerogen reactivity can also be seen in samples from the natural system, if such control is carefully looked for. Based on a large unpublished U.S. Geological Survey petroleum-geochemical data base for the Los Angeles, Ventura, and Southern San Joaquin Valley basins, intense hydrocarbon generation commences at burial temperatures of 120˚C–125˚C (vitrinite reflectance ≈0.6 percent), as reported by Phillipi (1965), in rocks containing type III organic matter (hydrogen index ≈300). Concurrently in these basins, in rocks having high hydrogen indices (and thus hydrogen-rich organic matter), commencement of hydrocarbon generation is not detected by Rock-Eval pyrolysis at highly elevated burial temperatures, for example, not by 200˚C in the Wilmington field, Los Angeles Basin (Price, 1983, figs. 3, 4), and not by 210˚C in the Shell Taylor 653 wellbore, Ventura Basin (Price, 1988, p. 31). In fact, all organic maturation indices are suppressed in rocks having high hydrogen indices, and, the higher the hydrogen index, the greater the degree of suppression of reaction extent for any given burial temperature range (figs. 12, 13). Vitrinite reflectance is perhaps the most widely used organic maturation index, and increases in the values of the Rock-Eval S_1 pyrolysis peak, and the transformation ratio, are easily measurable, direct consequences of C_{15}+ hydrocarbon generation. As shown in figures 12 and 13, as hydrogen index increases, the values of the three parameters discussed directly above strongly decrease. In the California petroleum basins, rocks having high hydrogen indices retain very immature characteristics to highly elevated burial temperatures and give no indication that they have commenced intense hydrocarbon generation at these burial temperatures.

Differences in reaction kinetics between different types of organic matter are also demonstrated by data from organic-geochemical studíes of deep wellbores (Price and others, 1979, 1981; Sagjo, 1980; Price, 1982, 1988; Price and Clayton, 1990). In these wells, an orderly progression of organic maturation proceeds with depth in thick sequences of rocks containing type III organic matter; kerogen burnout (loss of all hydrocarbon-generation potential) occurs in type III organic matter by vitrinite reflectance of 2.0 percent, as shown by zero, or near zero, hydrogen index values and by elemental hydrogen to carbon ratios for kerogen of 0.29–0.32 or less. With further increase in depth and passage

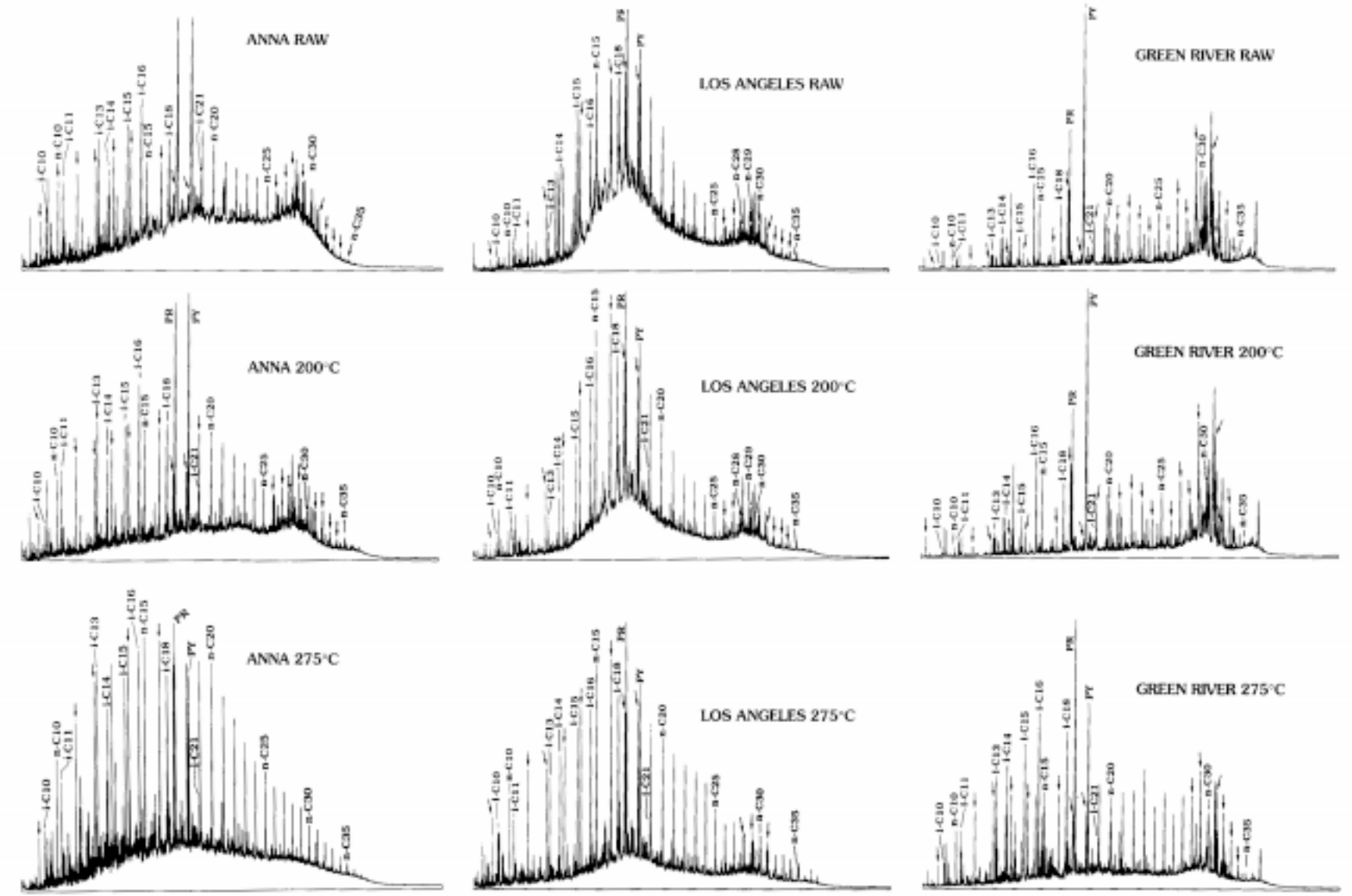

Figure 11. Gas chromatograms of C_8+ saturated hydrocarbons from the Middle Pennsylvanian Anna Shale Member, a mid-Miocene shale from the Los Angeles Basin, and shale from the Eocene Green River Formation from the raw (starting) rocks and from aqueous pyrolysis experiments of the rocks at 200˚C and 275˚C. Isoprenoid hydrocarbons are designated by i-c and the respective carbon number. PR, pristane; PY, phytane. N-paraffins are designated by n-c, and the respective carbon numbers and by arrows.

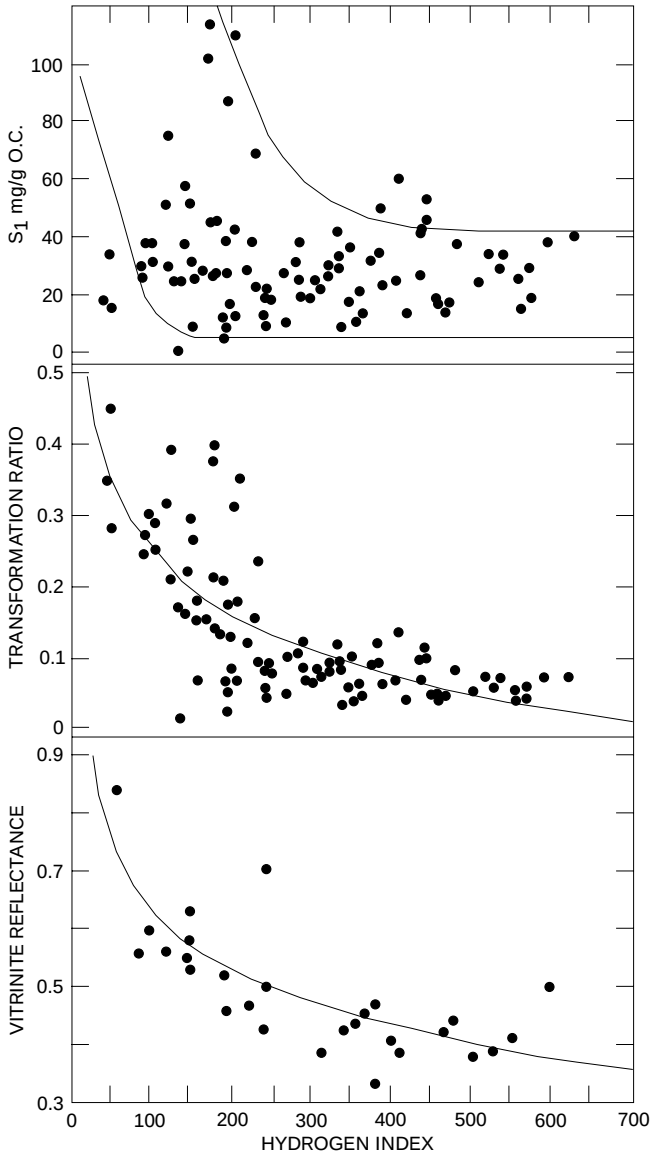

Figure 12. Vitrinite reflectance (R_o), Rock-Eval transformation ratio (S_1/S_1+S_2, also termed production index), and the S_1 pyrolysis peak (milligrams per gram organic carbon) versus hydrogen index for rocks from the California petroleum basins at equilibrium burial temperatures of 140˚C–159.9˚C. Samples are from the Ventura central syncline and the Ventura Avenue field of the Ventura Basin; from the Whittier, Long Beach, Wilmington, Santa Fe Springs, and Seal Beach fields of the Los Angeles Basin; from the Baldwin Hills community–1, the American Petrofina "Central C. H. –2" (central syncline, Los Angeles Basin), and the Long Beach Airport–1 wellbores; various wells in the Anaheim nose and northeast flank areas of the Los Angeles Basin; from various wells in the Paloma field, Southern San Joaquin Valley Basin; and from a well in the Santa Maria Valley Basin. All samples except for the American Petrofina and Santa Maria Valley Basin samples (cuttings chips) are core samples. The curved line in the vitrinite reflectance plot results from logarithmic regression analysis of the data and has a correlation coefficient of r=0.805 to the data. The line in the transformation ratio plot results from logarithmic regression analysis of the data and has a correlation coefficient of r=0.744 to the data. The lines in the S_1 pyrolysis peak plot define the principal sample population.

into rocks that were deposited under different conditions and that contain a marine-derived, more hydrogen rich organic matter, the hydrogen index and kerogen hydrogen to carbon ratio increase to moderate values. Furthermore, an entirely different maturation progression takes place in these rocks, as demonstrated by the data of the Foerster–1 wellbore (Price and Clayton, 1990). Thus, various maturation indices (whether measured from whole rocks, extracted bitumen, or macerated kerogen), after continuously increasing with depth in rock sequences containing type III organic matter, strongly reverse themselves to more immature values in passing into deeper rocks containing more hydrogen rich organic matter. Double-hydrocarbon-generation zones have been reported in sóme deep wells (Kontorovich and Trofimuk, 1976; Sagjo, 1980; Price and Clayton, 1990), the shallower zone being due to type III organic matter and the deeper zone presumably being due to more hydrogen rich organic matter. Lastly, the deep rocks in these wellbores retain measurable to moderate hydrocarbon-generation capacity (hydrogen index) to extreme maturation ranks, far past vitrinite reflectance of 2.0 percent, the thermal burnout for type III organic matter.

The Ralph Lowe–1 wellbore serves as an example (fig. 14). Kerogen in rocks shallower than 23,000 ft (7,010 m) in this well is dominated by vitrinite and inertinite (type III organic matter); however, the deepest rocks of this wellbore contain an overmature, hydrogen-rich organic matter made up mostly of amorphous kerogen (column A, fig. 14). The hydrogen index has values close to zero or zero at vitrinite reflectance ≥2.0 percent in this wellbore (column C, fig. 14), as is typical for type III organic matter (figs. 4 and 5). With the shift in organic matter type at well bottom to a more hydrogen rich organic matter, however, the hydrogen index dramatically increases. The behavior in the hydrogen index is mirrored by parallel changes in the kerogen atomic hydrogen to carbon ratio (column B, fig. 14). Dramatic increases in both C_{15}+ bitumen and C_{15}+ hydrocarbon concentrations accompany this shift in organic-matter type at depth in the wellbore (columns E and F, fig. 14).

Petroleum-geochemical data from another deep wellbore, the 31,464-foot (9,590 m)-deep Bertha Rogers–1, Washita County, Oklahoma, also demonstrate the control that organic-matter type has on hydrocarbon-generation reactions. Rocks from 0 to 17,514 ft (0–5,338 m) depth in this well contain type III organic matter. As such, both the hydrogen index and the kerogen hydrogen to carbon ratio progressively decrease with depth (fig. 15), and the hydrogen index projecting to zero values at about vitrinite reflectance of 2.0 percent (dashed line, column D, fig. 15), again typical behavior for type III organic matter. Lower

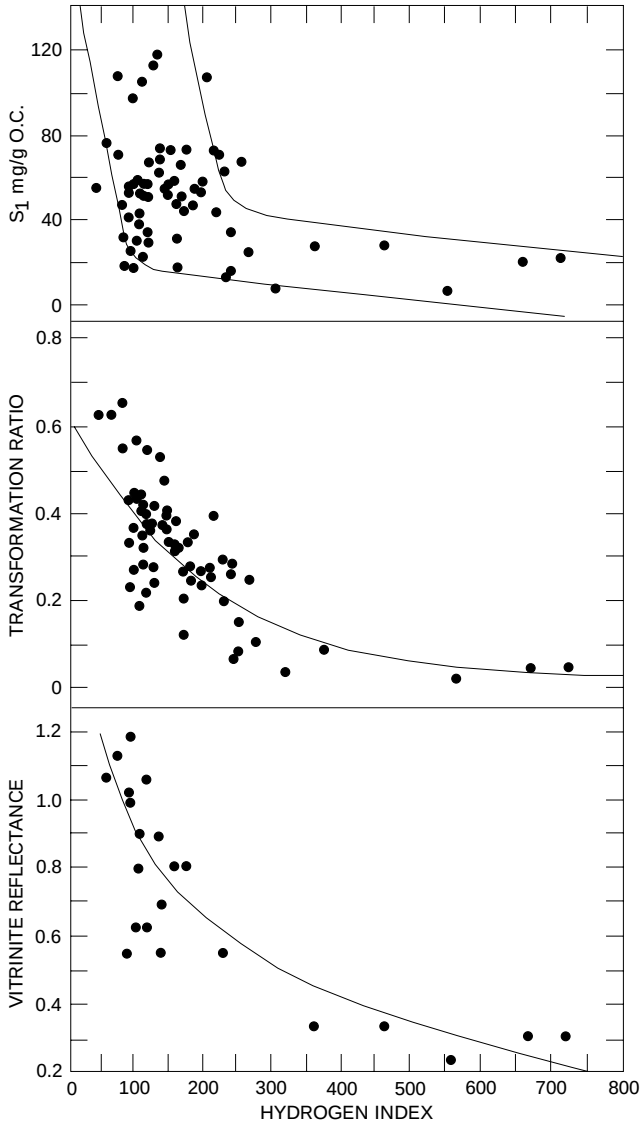

Figure 13. Vitrinite reflectance, Rock-Eval transformation ratio (S_1/S_2+S_2, also termed production index), and S_1 pyrolysis peak normalized to organic carbon (milligrams per gram organic carbon) versus the hydrogen index for rocks from the California petroleum basins and at equilibrium burial temperatures of 180˚C–199.9˚C. Samples are from the Wilmington field; the Houghton Community–1 (NW plunge Santa Fe Springs field); and the American Petrofina "Central C.H.–2" (all Los Angeles Basin); and from the Paloma field, Southern San Joaquin Valley Basin. The curved line in the vitrinite reflectance plot results from logarithmic regression analysis of the data and has a correlation coefficient of r=0.867 to the data. The lines in the S_1 pyrolysis peak plot define the principal sample population.

Pennsylvanian (Morrowan) and older rocks (17,514 ft, 5,338 m, and deeper) were deposited, however, under more marine conditions and as such contain a more hydrogen rich organic matter than the shallower rocks. Hence, both the hydrogen index and the kerogen atomic hydrogen to carbon ratio increase in the deeper rocks (columns B and D, fig. 15). With further increase in depth, the kerogen hydrogen to carbon ratio again continuously decreases to low values (0.25–0.30) at well bottom. The behavior of the hydrogen index in the deeper rocks is clouded by a large-scale expulsion of bitumen generated by the organic-rich shale of the Woodford Shale (Upper Devonian and Lower Mississippian) into the adjacent organic-poor rocks. The Rock-Eval analysis includes the resins and asphaltenes in this migrated bitumen in the S_2 pyrolysis peak. Thus, the elevated hydrogen index at depth does not reflect the true hydrocarbon-generation capacity (which would be low) of these organic-poor rocks, if the rocks were Soxhlet extracted.

Accurate comparisons of reaction kinetics for the different organic-matter types from natural samples have previously been obfuscated by the fact that it is very difficult to obtain valid maturation-rank estimates that can be directly related to vitrinite reflectance or paleo-burial temperature from natural samples that contain types I and II organic matter. It is now recognized that vitrinite reflectance in types I and II organic matter is suppressed at any rank as compared to that in type III organic matter (Price and Barker, 1985). However, all maturation reactions, including vitrinite reflectance, proceed at slower rates for any given thermal history in sulfur-poor, hydrogen-rich organic matter than in type III organic matter buried under the same conditions (Price, 1991). Thus, it is not now possible to assign accurate maturation ranks to sections of rocks that do not contain type III organic matter, such as the Jurassic section of the Paris Basin, the Jurassic through Lower Cretaceous section of the Greater Gulf Coast, and the uppermost Cretaceous through Eocene section in the Uinta Basin. In my opinion, the true maturity of carbonate-evaporite sections presently cannot be estimated with any confidence.

The preceding discussion demonstrates that organic-matter type has a dominant control on hydrocarbon generation. Hydrogen-rich types I and II organic matter both require higher burial temperatures to commence hydrocarbon generation than does type III organic matter, and they also retain measurable (and sometimes moderate to high) hydrocarbon-generation potential to much higher ranks than does type III organic matter. The bearing that these conclusions have on high-rank gas deposits is discussed in Price (this volume).

ALTERNATE RANKS FOR SOME PETROLEUM-GEOCHEMICAL EVENTS

As stated, the vitrinite reflectance-event pairs of figure 1 are accepted as geochemical law; however, that a large body of published data does not fall within the constraints of figure 1 suggests that significant problems may exist with figure 1. Figure 4 provides insight to this point. The S_1

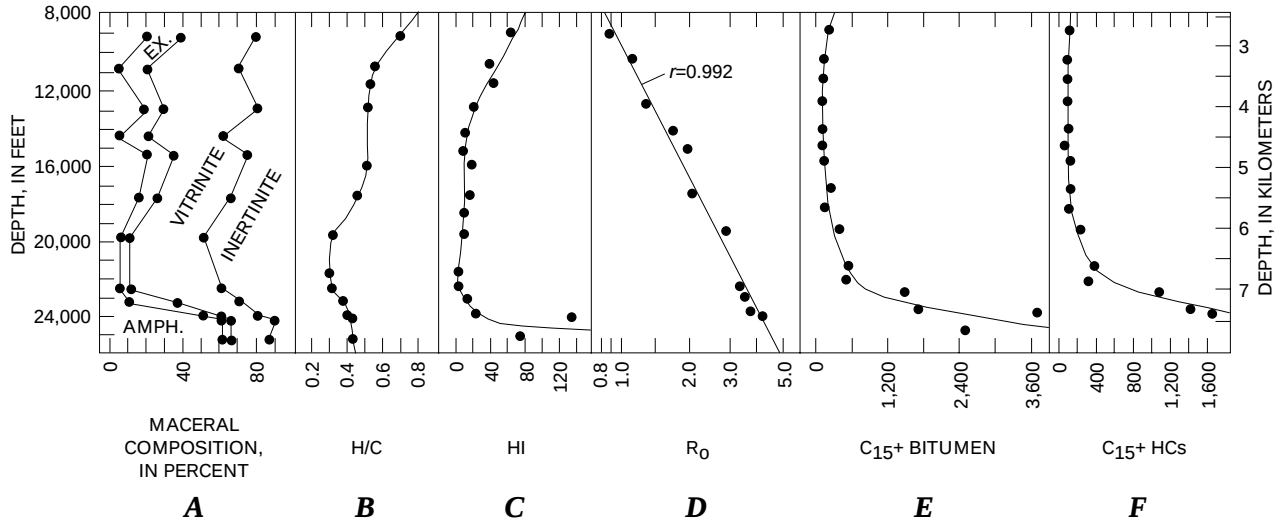

Figure 14. Petroleum-geochemical data from the Ralph Lowe–1 wellbore, Pecos County, Texas, versus depth. *A*, Maceral analyses of isolated kerogen by Robertson Research; EX., exinite; AMPH., amorphous. *B*, Atomic hydrogen to carbon ratio for isolated kerogen. *C*, Rock-Eval hydrogen index for Soxhlet-extracted powdered rock. *D*, Vitrinite reflectance (in percent). The straight line in this plot has a correlation coefficient (*r*) of 0.992 to the data. *E*, C_{15}+ bitumen (in parts per million by rock weight). *F*, C_{15}+ hydrocarbons (in parts per million by rock weight).

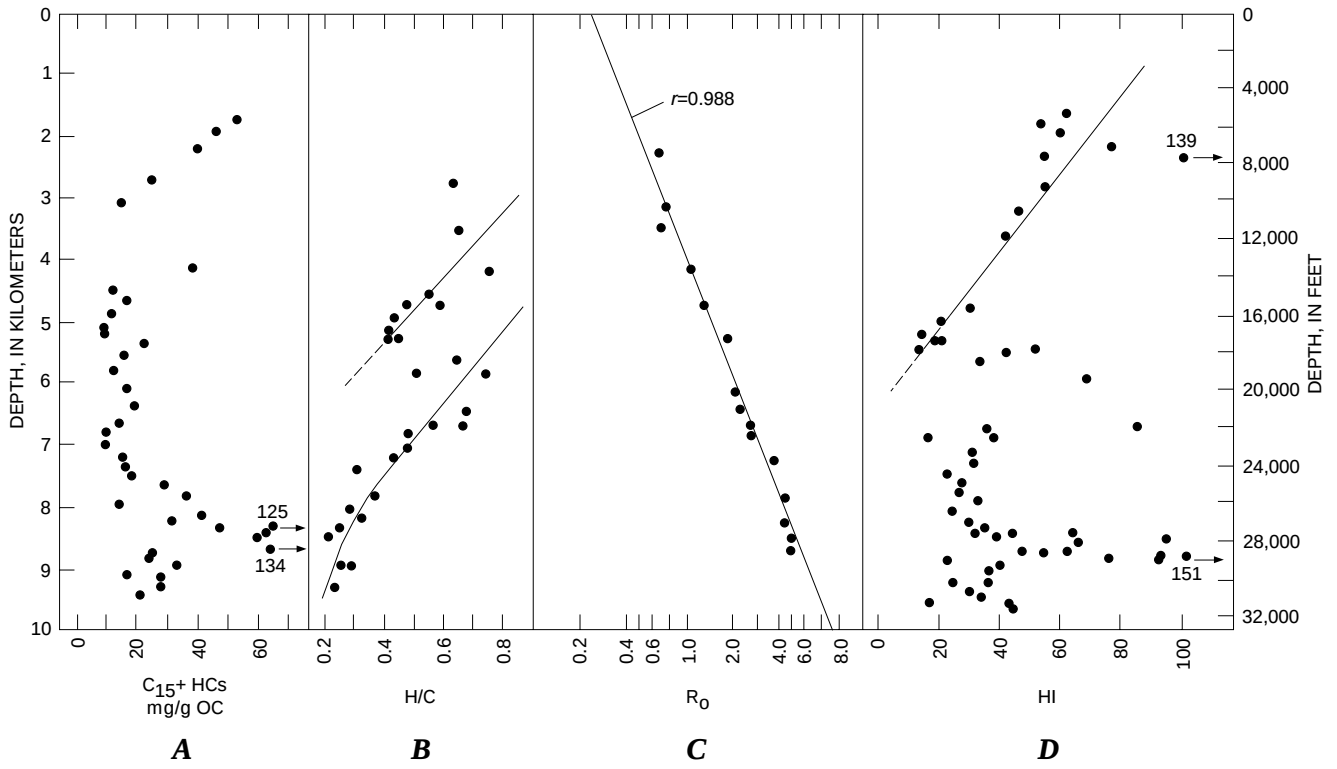

Figure 15. Petroleum-geochemical data from the Bertha Rogers–1 wellbore, Washita County, Oklahoma, versus depth. *A*, Milligrams of C_{15}+ hydrocarbons per gram of organic carbon. *B*, Atomic hydrogen to carbon ratio for isolated kerogen. *C*, Vitrinite reflectance (in percent); the straight line in this plot has a correlation coefficient (*r*) of 0.988 to the data. *D*, Rock-Eval hydrogen index.

pyrolysis peak is a measure of C_{15}+ hydrocarbon generation. Thus, the increase in S_1 pyrolysis peak values (fig. 4) at R_o=0.6 percent (due to an increase in Soxhlet-extractable hydrocarbons) results from the commencement of hydrocarbon generation. This increase in C_{15}+ hydrocarbons at R_o=0.6 percent is equated to the first possibility of

commercial-oil deposits. The maximum in the S_1 pyrolysis peak at R_o=0.9 percent has been equated to the maximum in hydrocarbon generation, and C_{15}+ hydrocarbon-thermal destruction occurs at higher vitrinite reflectance values. C_{15}+ hydrocarbon-thermal destruction previously was thought to be complete by R_o=1.35 due to the low values of both the S_1 pyrolysis peak and Soxhlet-extractable hydrocarbons in coal and rock containing type III organic matter at this rank; however, the coals of figure 4 at R_o ≥1.35 percent still have high hydrogen index values and thus significant hydrocarbon-generation capacity. Furthermore, pyrolysis-gas chromatography (Teichmüller and Durand, 1983) on some of the high-rank coals of figure 4 demonstrates that part of this generation capacity is for C_{15}+ hydrocarbons (approximately 37 percent for coals at R_o=1.35 percent, fig. 16). Clearly, the bonds broken in hydrocarbon generation are weaker than those broken in hydrocarbon-thermal destruction. Thermodynamic or kinetic models are simply not possible wherein C_{15}+ hydrocarbons can be thermally destroyed before they are generated. Thus the data of figures 4, 5, and 16 demonstrate that the low S_1 pyrolysis peak values at R_o ≈1.35 percent must be due to causes other than hydrocarbon-thermal destruction.

Those causes are most probably primary migration by gaseous solution and loss of generated hydrocarbons to drilling mud as the rock moves up the wellbore in drilling operations. In figure 4, hydrocarbon concentrations (S_1 pyrolysis peak) increase at R_o=0.6 percent from commencement of hydrocarbon generation; however, *intense* hydrocarbon generation commences with the first noticeable decrease in the maximal hydrogen-index values of the coals, at R_o=0.8 percent. Aqueous-pyrolysis experiments of Wenger and Price (1991) demonstrate that with commencement of intense hydrocarbon generation in type III organic matter, intense generation of hydrocarbon gases also commences and, thus, intense primary migration by gaseous solution (Price, 1989a, b). Such a migration contributes to the decrease in hydrocarbon concentrations observed in type III organic matter at R_o ≥0.8–0.9 percent.

The greatest loss of generated hydrocarbons results, however, from the large pressure decreases that occur as rock moves up the wellbore in drilling operations, especially when rocks contain gas-prone type III organic matter. This

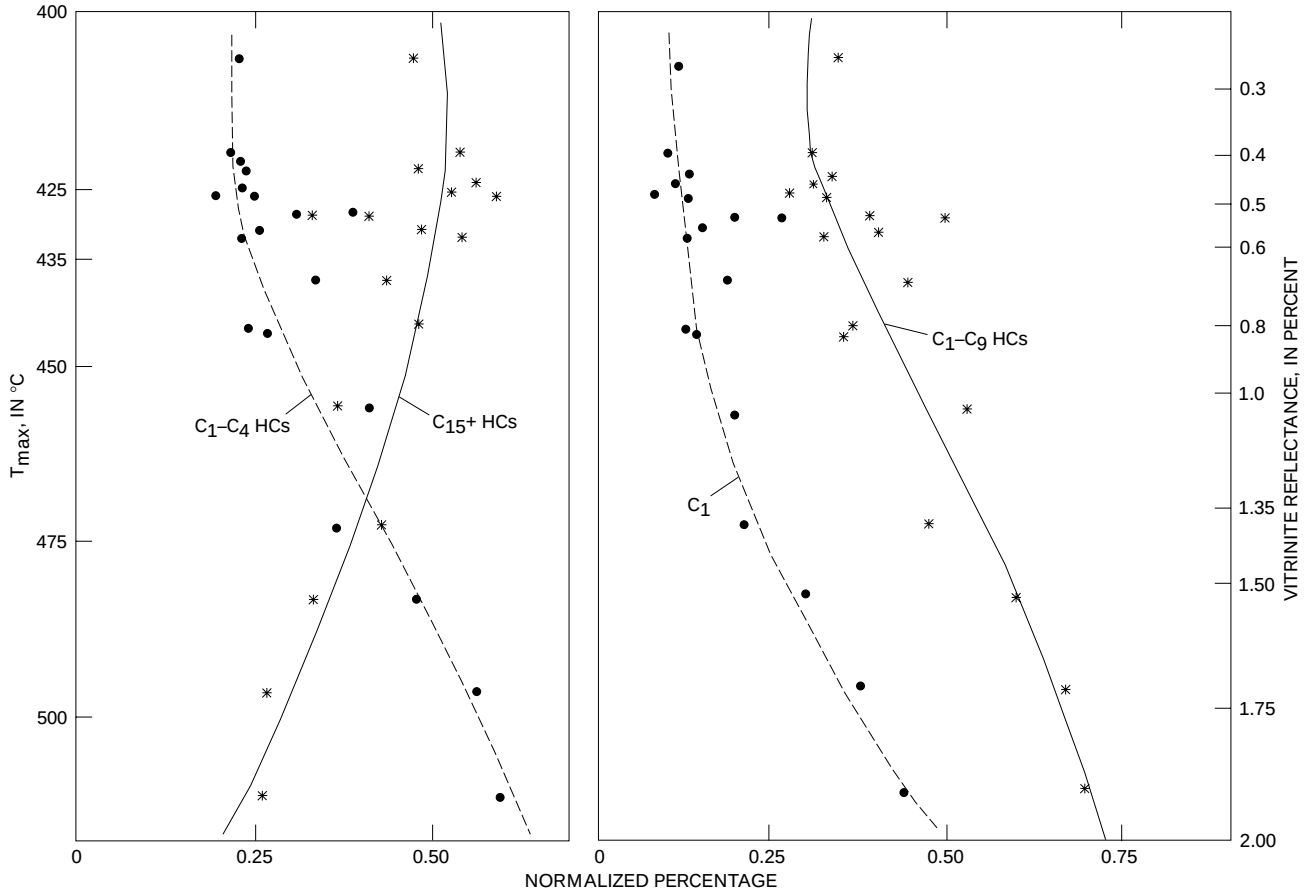

Figure 16. Composition of products from thermal vaporization of coals (Rock-Eval pyrolysis, product trapping, and gas chromatography). Vitrinite reflectance values (R_o) derived from T_{max} values by use of table 1 in Price (1989b). Data from Teichmüller and Durand (1983). The original vitrinite reflectance data were given as R_m values; R_m was converted to R_o by R_m=1.066R_o.

hydrocarbon loss is discussed in some detail in Price and LeFever (1992) but is reviewed here. Price and Clayton (1992) demonstrated that a crude-oil-like phase is prefractionated from the whole bitumen in organic-rich source rocks and is concentrated in cracks and parting laminae in such rocks ready for expulsion. As conventional core and cuttings chips ascend the wellbore during drilling operations, these rocks undergo large fluid-pressure decreases, from high formation pressures at depth to atmospheric pressure at the wellhead. Deep (25,000 ft, 7,620 m) Gulf Coast shales, for example, suffer pressure decreases from 20,000–24,000 psi at depth to less than 15 psi at wellhead. Gases present both in the rocks and in the bitumen in the rocks greatly expand in volume as pressure decreases in partial response to the ideal gas law $PV=nRT$ and almost totally exit from the rocks to the drilling muds. Such gases, moving from interior rock volumes, blow out oil like bitumen concentrated in parting laminae and fractures into the drilling mud. Sokolov and others (1971) provided insight into the magnitude of this hydrocarbon-gas loss (table 2). They took rock samples at depth and at formation pressure in what they termed the "KC lifter" (a pressure core barrel sampler) and brought the samples to the surface, sealed and at formation pressure, with no gas loss. They compared the amount of gas recovered in this manner to that recovered during an open-hole rock trip up the wellbore, where only 0.11–2.13 percent of the gas originally in the rock was recovered.

Observations by wellsite geologists and drilling personnel corroborate the results of Sokolov and others (1971). Cuttings chips of organically mature, fine-grained rocks violently spin and fizz at wellhead from outgassing of only the gas remaining in the rocks at wellhead, which is but a small fraction of the gas originally present in the rock, before the trip up the wellbore. During drilling through mature organic-rich rocks, mud-gas-logging values always dramatically increase from the outgassing of these rocks into the drilling mud. Occasionally, the logging results from such shales are deleted because they are so large as to overshadow values from possible gas-bearing, coarse-grained rocks. Mud-fluorescence values obtained during drilling through organic-rich, mature, fine-grained rocks also always dramatically increase due to the effusion of oil-like bitumen from these rocks into the drilling mud. During drilling of mature shales of the Bakken Formation (Upper Devonian and Lower Mississippian) in the Williston Basin with a water-based drilling mud, an oil film always covers the mud pit. Source-rock cores crackle in the core barrel from gas loss at wellhead or bleed oil while being held at wellhead and can continue to bleed oil long after while sitting in the laboratory. This hydrocarbon loss is enhanced during drilling operations because cores, and especially cuttings chips, are highly disrupted by the drill bit. Although many petroleum geochemists do not appreciate the magnitude of this hydrocarbon loss from mature source rocks during the rock trip uphole, this large hydrocarbon loss from mature source rocks has been well known to well-site geologists for more than 40 years (C.W. Spencer, U.S. Geological Survey, written commun., 1991).

Table 2. Hydrocarbon gas concentration and relative loss from equivalent core samples using the "KC core lifter" and the normal "open"method.
[From Sokolov and others (1971)]

Rock type	Sample depth (feet)	Sample mode	Concentration ($\times 10^{-4}$cm^3/kg rock)	Relative loss (KC/open)
Sand	1,263	KC	106,243	893
		Open	119	
Shale	1,887	KC	2,431	47
		Open	52	
Shale	2,034	KC	36,473	529
		Open	69	

It is maintained herein that the hypothesized thermal deadline of C_{15}+ hydrocarbons at R_o=1.35 percent (1) is incorrect and (2) originated from an assignation of the decrease of C_{15}+ hydrocarbon concentrations in type III organic matter at $R_o \geq 0.9$ percent to hydrocarbon-thermal destruction. This decrease is most probably due to primary migration and hydrocarbon loss to drilling mud during the rock trip uphole in drilling operations.

The data of figure 4 suggest alternate ranks to those of figure 1 for important petroleum-geochemical events in type III organic matter. Hydrocarbon generation does commence by R_o=0.6 percent; however, intense hydrocarbon generation and primary migration commence at R_o=0.8 percent and mostly occur from R_o=0.9 to 1.6 percent, a range in which the greatest decrease in hydrogen index occurs (figs. 4, 5). Hydrocarbons cannot form oil deposits until they leave the source rocks (expulsion), and expulsion commences at R_o=0.9 percent and corresponds to the significant decrease in the S_1 pyrolysis peak values at that rank. Thus, R_o=0.9 percent would be a better estimate than R_o=0.6 percent for the first possibility of commercial-oil deposits. Type III organic matter loses most or all hydrocarbon-generation potential by R_o=2.0 percent (zero or near zero hydrocarbon index; figs. 4, 5). This vitrinite reflectance level is not equivalent to C_{15}+ hydrocarbon-thermal destruction because types I and II organic matter retain remnant to moderate hydrocarbon-generation potential to much higher ranks (discussed preceding and following).

HYDROCARBON THERMAL STABILITY LIMITS

In this study, three approaches were taken to examine hydrocarbon thermal-stability limits: (1) examination of quantitative and qualitative changes, versus maturation rank, in hydrocarbons from rocks that were at high paleo-burial temperatures in deep wellbores; (2) examination of organic products from aqueous-pyrolysis experiments performed at temperatures high enough to result in hydrocarbon-thermal

destruction; and (3) examination of qualitative changes in hydrocarbon compositions of gas condensates or light oils previously exposed to high paleo-burial temperatures.

DEEP WELLBORE DATA

Detailed petroleum geochemistry of high-rank rocks (table 3) from deep (22,000–30,000 ft, 6,700–19,145 m) wellbores (Kontorovich and Trofimuk, 1976; Price and others, 1979; Sagjo′, 1980; Price and others, 1981; Price, 1982; Guthrie and others, 1986; Price, 1988; Price and Clayton, 1990) demonstrates that moderate to high concentrations of both C_{15}+ hydrocarbons and C_{15}+ bitumen (fig. 17) can persist to elevated maturation ranks (vitrinite reflectance=2.0–7.0 percent). Such data do not conform to the hypothesis of a thermal destruction of C_{15}+ hydrocarbons by R_o=1.35 percent. Some investigators have attributed the data of figure 17 as simply due to caving or contamination by organic-based drilling fluids. These possibilities were thoroughly discussed (and dismissed) in each of the above publications. Singular compositional characteristics of the high-rank hydrocarbons, or of the rocks from which they were derived, for all the wells of table 3 demonstrate that the measured high-rank hydrocarbons were indigenous. The data from the Ralph Lowe–1 well (discussed preceding, fig. 14) serve as an example of this point, and data from the Chevron R.G. Jacobs–1, Goliad County, Texas (fig. 18), serve as another example.

In figure 18, Tertiary rocks shallower than 14,000 ft (4,270 m) all contain type III organic matter, and the expected increase in C_{15}+ bitumen for type III organic matter is evident at R_o=0.6 percent, as is a maximum in the bitumen coefficient at R_o=0.9 percent, and decreasing values at higher ranks. As is characteristic of type III organic matter, by R_o=2.00 percent the Tertiary rocks have lost all hydrocarbon-generation capacity as shown by the low and decreasing hydrogen indices at those ranks. (The low hydrogen index for the sample at 3,000 ft [914 m] [R_o=0.5 percent] is from original depositional conditions and is not a result of organic-matter metamorphism.) At the top of the Lower Cretaceous section (wavy lines in total organic carbon and hydrogen index plots, fig. 18), depositional conditions different from those of the Tertiary rocks resulted in a marine type II organic matter in the deeper rocks. This is demonstrated by the elevated hydrogen index for the five Gulfian Series samples (dots below the wavy line, hydrogen index plot fig. 18). These elevated hydrogen index values at R_o=1.7–3.0 percent (1) are from ground shales that were Soxhlet-extracted for 48 hours prior to Rock-Eval analysis, (2) are representative of hydrocarbon-generation potential indigenous only to the rock, and (3) clearly do not conform to the hypothesis of thermal destruction of C_{15}+ hydrocarbons by R_o=1.35 percent.

The crosses at depths of 21,000 ft (6,400 m) and greater in figure 18 represent core samples from a low-porosity,

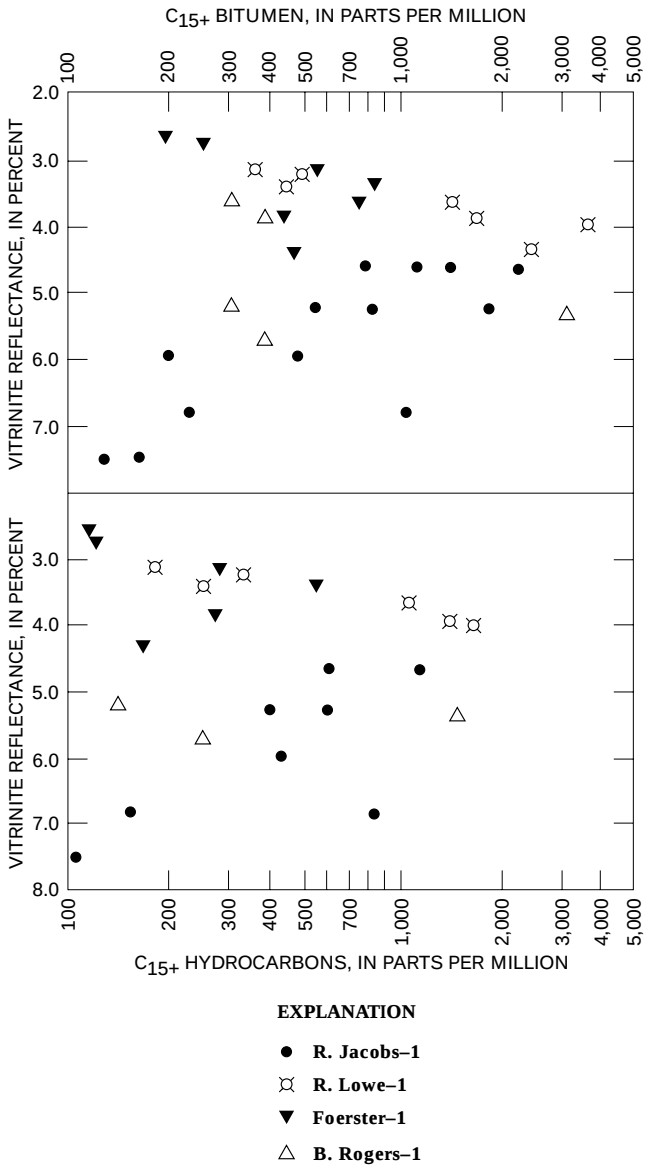

Figure 17. C_{15}+ bitumen and C_{15}+ saturated plus aromatic hydrocarbons from Soxhlet-extracted deep rocks of Bertha Rogers–1, R.G. Jacobs–1, Ralph Lowe–1, and A.M. Foerster–1 wellbores versus vitrinite reflectance (table 1). Data are from table 4.

low-permeability carbonate rock that was heavily oil stained as shown by residual oil saturation analyses (fig. 19) performed by Core Labs. This oil staining (1) causes the high bitumen coefficients (fig. 18) in rocks at R_o=4.25–6.5 percent and at present-day burial temperatures of 250˚C–282˚C and (2) provides incontrovertible evidence of the thermal stability of C_{15}+ hydrocarbons to extreme maturation ranks in highly pressurized, tight, fine-grained (closed-system) rocks. The data of figures 18 and 19 have been replicated by several laboratories other than those of the U.S. Geological Survey, Core Labs, and Chevron Oil Field Research.

Table 3. List of wells used for figure 17.
[Vitrinite reflectance (R_o) is extrapolated Ro at well bottom based on depth versus R_o plots, all of which have correlation coefficients <0.99]

Well and location	Depth (meters)	R_o (percent)	Range of rock ages penetrated in wellbore	Reference
Lone Star Bertha Rogers–1, Washita County, Oklahoma	9,583.7	8.0	Permian-Cambrian	Price and others (1981).
Ralph Lowe–1, Pecos County, Texas	8,686.4	5.8	Permian-Ordovician	Price 1988).
Shell McNair–1, Hinds County, Mississippi	6,911.0	2.8	Early Tertiary-Jurassic	Price and others (1979).
Chevron Jacobs–1, Goliad County, Texas	7,546.8	7.5	Miocene–Early Cretaceous	Price (1982).
Pan Am Clayton Foester–1, La Salle County, Texas	6,703.7	7.0	Early Tertiary–Jurassic	Price and (1990).

Table 4. Geological and geochemical data for four wells cited in this study
[C15+ BIT (C15+ bitumen) is in parts per million by rock weight and normalized to organic carbon (mg/g OC); C15+ HCs (C15+ hydrocarbons) is in parts per million by rock weight and normalized to organic carbon (mg/g OC). Burial temperatures for the Foerster–1 are based on an estimated regional geothermal gradient for La Salle County, Texas, of 36.7∞C/km]

Depth	Vitrinite reflectance	C_{15}+ BIT		C_{15}+ HC		Total organic	Present-day burial	
(meters)	(percent)	(ppm)	(mg/g OC)	(ppm)	(mg/g OC)	carbon	temperature (°C)	Geologic age
Foerster–1								
4,602–4,724	2.58	193	80	114	48	0.24	196	Early Cretaceous.
4,724–4,846	2.73	252	105	118	49	0.24	201	Early Cretaceous.
4,968–5,151	3.10	556	132	280	67	0.42	211	Early Cretaceous.
5,151–5,334	3.36	828	172	545	114	0.48	218	Jurassic.
5,334–5,456	3.60	740	154	476	99	0.48	224	Jurassic.
5,456–5,578	3.80	442	108	271	56	0.41	228	Jurassic.
5,761–5,882	4.37	467	31	165	11	1.51	238	Jurassic.
Ralph Lowe–1								
6,026–6,032	3.08	358	26	179	13	1.39	187	Pennsylvanian.
6,629–6,635	3.20	500	37	332	25	1.34	204	Pennsylvanian.
6,882–6,888	3.38	451	14	251	8	3.08	211	Pennsylvanian.
7,080–7,087	3.57	1,410	41	1,030	30	3.46	216	Mississippian.
7,324–7,330	3.86	1,650	38	1,380	32	4.32	223	Mississippian.
7,391–7,398	3.93	3,590	151	1,610	68	2.87	225	Mississippian.
7,718–7,724	4.30	2,420	90	NA	NA	2.68	234	Devonian.
R. G. Jacobs–1								
6,400.8	4.60	2,200	176			1.25	254	Early Cretaceous.
6,401.7	4.60	1,400	303	1,100	239	0.46	254	Early Cretaceous.
6,407.7	4.61	1,100	105			1.05	255	Early Cretaceous.
6,418.3	4.61	776	141	588	107	0.55	255	Early Cretaceous.
6,698.7	5.22	1,800	367			0.49	265	Early Cretaceous.
6,705.8	5.22	805	267	590	174	0.34	266	Early Cretaceous.
6,711.2	5.23	548	261	398	189	0.21	266	Early Cretaceous.
7,000.0	5.95	200	74			0.27	276	Early Cretaceous.
7,005.7	5.95	483	172	365	130	0.28	276	Early Cretaceous.
7,297.7	6.80	1,025	214	844	176	0.48	286	Early Cretaceous.
7,313.8	6.81	230	74	153	49	0.31	288	Early Cretaceous.
7,539.1	7.50	165	72	104	45	0.23	296	Early Cretaceous.
7,544.6	7.51	129	64	65	33	0.20	296	Early Cretaceous.
Bertha Rogers–1								
8,357–8,378	5.20	306	278	140	145	0.11	224	Mississippian.
8,442–8,470	5.30	3,010	84	1,450	60	3.59	226	Miss.–Devonian.
8,558–8,723	5.70	389	162	252	134	0.24	230	Devonian.

The high concentrations of both C_{15}+ hydrocarbons and C_{15}+ bitumen (fig. 14, columns E and F), in the deep, high-rank rocks containing hydrogen-rich organic matter in the Ralph Lowe–1 wellbore also demonstrate that C_{15}+ hydrocarbons are thermally stable to much higher maturation ranks than represented by the paradigm of figure 1. It should

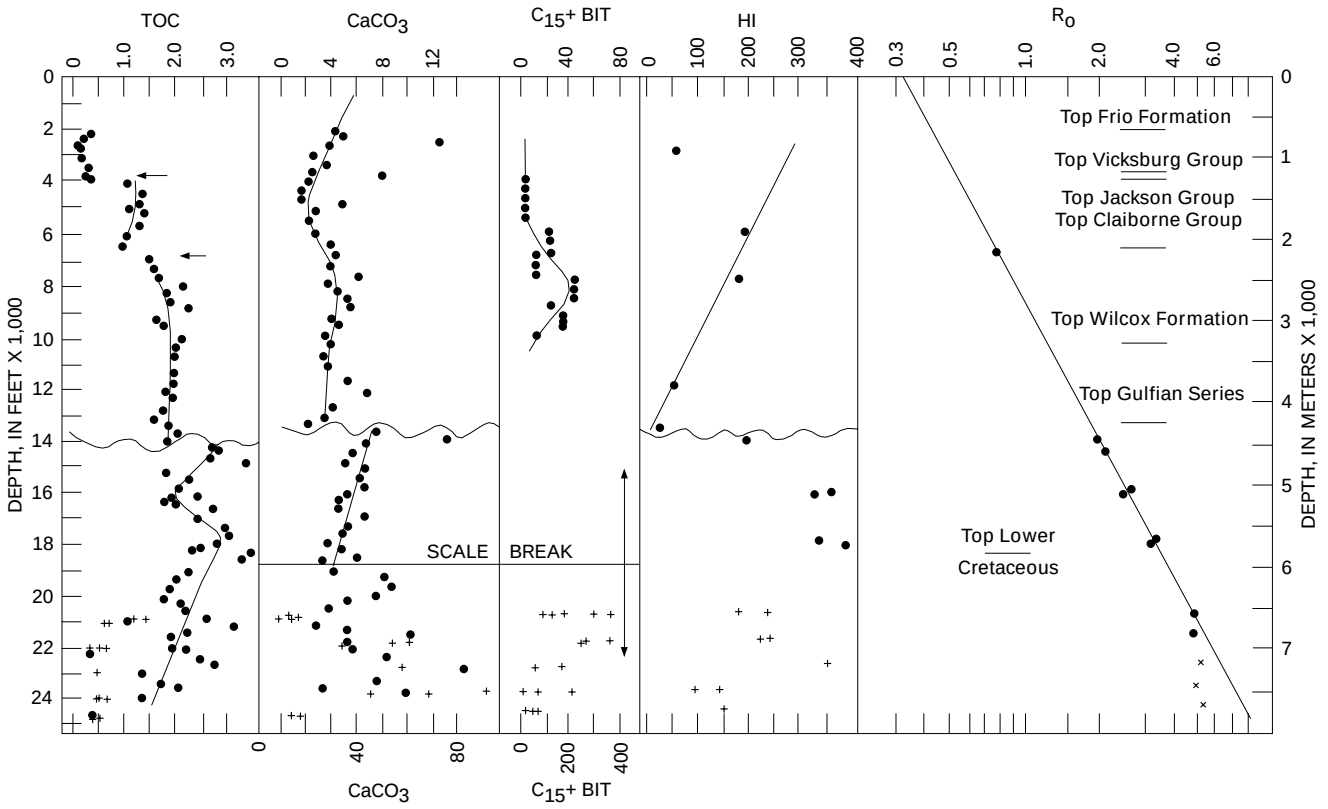

Figure 18. Various petroleum-geochemical parameters versus depth for Chevron R.G. Jacobs–1 wellbore, Goliad County, Texas. Total organic carbon (TOC) and calcium carbonate ($CaCO_3$) contents in weight percent; C_{15}+ bitumens (C_{15}+ BIT) (by Soxhlet extraction) in milligrams per gram of organic carbon; HI (Rock-Eval hydrogen index); and vitrinite reflectance (R_o, in percent). Arrows in TOC plot delineate sharp increases in total organic carbon at stratigraphic boundaries. Wavy lines signify a lithologic depositional break at the Tertiary-Cretaceous boundary. Solid lines in the $CaCO_3$ and C_{15}+ bitumen plots signify a scale break (at the Upper Cretaceous–Lower Cretaceous boundary) for these two plots; $CaCO_3$ and bitumen scales on top of figure serve for samples above this line; scales on bottom of figure serve for samples below this line. "X's" in the R_o plot represent vitrinite reflectance values that probably have some degree of suppression.

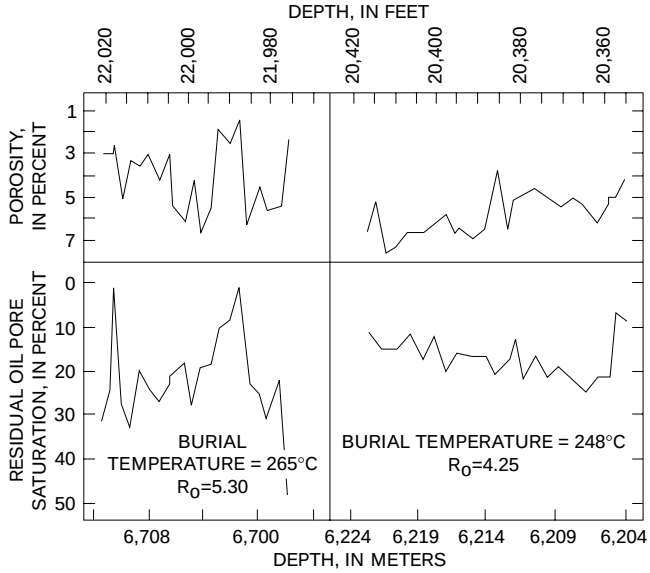

Figure 19. Percent porosity and percent residual oil pore saturation versus depth for two of the deep cored intervals of the R.G. Jacobs–1 wellbore (table 1). Analyses by Core Labs; data supplied by Chevron Oil Field Research Company.

be noted that the deep rocks from the Ralph Lowe–1 wellbore also retain significant hydrocarbon-generation potential (as reflected by their hydrogen index values) even to these extreme ranks, also demonstrating that types I and II organic matter can retain significant remnant hydrocarbon-generation potential to much higher maturation ranks than type III organic matter.

COMPOSITIONAL CHANGES IN SATURATED HYDROCARBONS AT DESTRUCTION

Compositional changes in saturated hydrocarbons during their thermal destruction are better appreciated by briefly reviewing gross compositional changes in saturated hydrocarbons during hydrocarbon generation. The gas chromatograms of figure 20 are from aqueous-pyrolysis experiments performed on carbonaceous shale of the Middle Pennsylvanian Anna Member. The unreacted rock has total organic carbon contents of 23–25 percent and contains type III/II organic matter (hydrogen index 320). Typically, immature

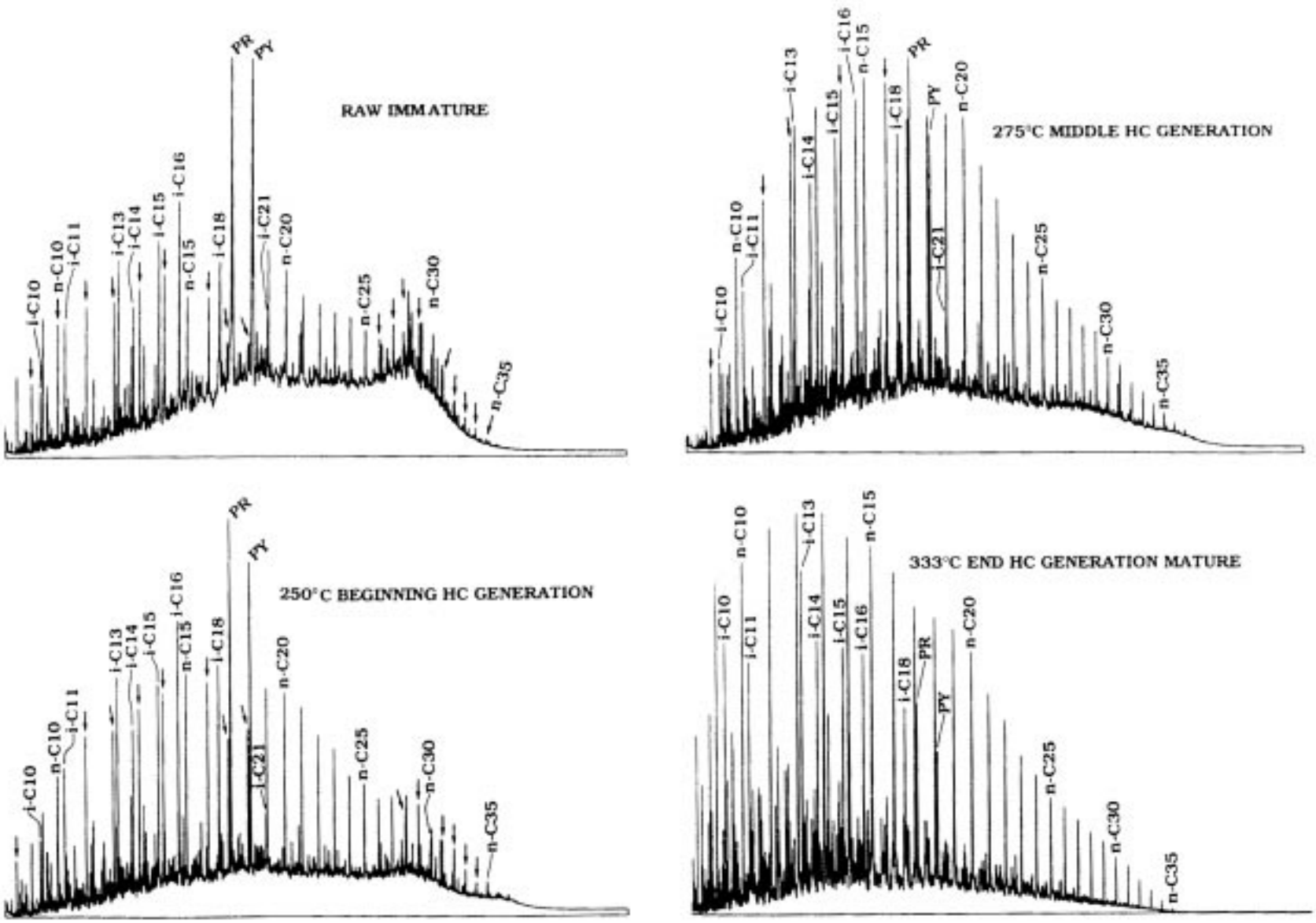

Figure 20. Gas chromatograms of C_8+ saturated hydrocarbons generated by aqueous pyrolysis of carbonaceous shale from the Middle Pennsylvanian Anna Shale Member. Every fifth n-paraffin is labeled by n-C with its respective carbon number. N-paraffins are also labeled by arrows when necessary. Isoprenoid hydrocarbons are labeled by i-C with their respective carbon number. PR, pristane; PY, phytane; HC, hydrocarbon.

(pre-hydrocarbon generation) saturated hydrocarbons have (with some variance due to organic-matter type) (fig. 20) (1) bimodal distributions in large naphthenic envelopes, (2) low concentrations of n-paraffins relative to adjacent isoprenoid hydrocarbons, (3) large biomarker peaks (in the carbon number range 26–32) relative to adjacent n-paraffins, (4) an irregular n-paraffin profile (distribution), and (5) low concentrations of C_{15-} hydrocarbons. During hydrocarbon generation, these characteristics progressively change (fig. 20), and gas chromatograms of mature saturated hydrocarbons have (1) small naphthenic envelopes with unimodal distributions, (2) n-paraffins with a regular profile and in high concentrations relative to both adjacent isoprenoid hydrocarbons and biomarker peaks, and (3) high concentrations of C_{14} hydrocarbons.

Changes in saturated hydrocarbons during thermal destruction are demonstrated by the gas chromatograms of figure 21 from aqueous-pyrolysis experiments on the shale of the Retort Member of the Lower Permian Phosphoria Formation and on a hydrogen-poor lignite. The Phosphoria shale sample, run at 350˚C and 1,077 bars, is in the middle of main-stage saturated hydrocarbon-thermal destruction. As such, total C_5+ extractables have decreased to 83 mg/g rock from 161 mg/g of rock at the next lowest experimental level (333˚C, 80.8 bars). In the gas chromatogram of the 350˚C, 1,077-bar sample, the thermally labile isoprenoid hydrocarbons, especially pristane and phytane, are in greatly reduced concentrations relative to their adjacent n-paraffins (compare to the 333˚C Anna Shale chromatogram, fig. 20). Furthermore, the concentration of each isoprenoid hydrocarbon decreases with increase in isoprenoid-hydrocarbon carbon number. Also, the naphthenic envelope is quite small, and the smooth logarithmic n-paraffin distribution suggests that a kinetic or thermodynamic (metastable?) equilibrium has been established within the n-paraffins. In another 350˚C Phosphoria shale experiment, system pressure was decreased from 1,077 bars to 119 bars, thus illustrating the effect of increasing fluid pressure on retarding organic-matter metamorphism. The 119-bar sample is near the end of saturated-hydrocarbon thermal destruction, and C_5+ extractables have decreased to 31 mg/g rock from 83 mg/g rock in the 350˚C, 1,077-bar sample. The isoprenoid-hydrocarbon peaks are in reduced concentrations; note the absence of pristane and phytane. The isoprenoid hydrocarbons, and all other peaks between the n-paraffins, decrease in concentration with increasing carbon number. The concentrations of the C_{25}+ n-paraffins are also reduced in the 119-bar sample as compared to those in the gas chromatogram from the 1,077-bar sample, and there is almost no naphthenic envelope.

The lignite run at 350˚C and 125 bars is at the end of C_{15}+ saturated-hydrocarbon thermal destruction. Comparison of the gas chromatogram of this sample with the chromatogram of the Phosphoria 350˚C, 119-bar experiment demonstrates the effect of product escape on organic-matter metamorphism. The hydrogen-poor lignite (hydrogen index of 55 for unreacted rock) has a low hydrocarbon-generation capacity as compared to the hydrogen-rich organic matter in the Phosphoria shale (hydrogen index of 450 in the unreacted rock). The 350˚C, 125-bar lignite and 350˚C, 119-bar Phosphoria Shale experiments were run essentially under the same conditions; however, the C_{15}+ saturated hydrocarbon concentration in the lignite experiment was 0.19 mg/g rock as compared to 3.85 mg/g rock in the Phosphoria shale experiment. The low concentration of saturated hydrocarbons (and total bitumen) in the lignite experiment allowed saturated-hydrocarbon thermal destruction to proceed further as compared to similar experiments with more organic-rich rocks. As such, in the lignite chromatogram, (1) all C_{27}+ saturated hydrocarbons have been thermally destroyed, (2) peaks other than the n-paraffins are in very small concentrations, (3) no naphthenic envelope is present, and (4) the n-paraffins make up 95–99 percent of the sample.

In the 375˚C, 132-bar experiment on the Phosphoria shale, the thermal deadline for C_{15}+ saturated hydrocarbons had been passed, and all C_{14}+ saturated hydrocarbons were destroyed.

Saturated hydrocarbons have the following characteristics during their thermal destruction as delineated by the aqueous-pyrolysis experiments of Wenger and Price (1991) and Price and Wenger (1991). The thermally unstable, 4- and 5-ringed naphthenic hydrocarbons crack first, followed by the isoprenoid hydrocarbons, and then the iso-alkanes. The n-paraffins are the most stable of the common saturated hydrocarbons. This fact was also noted by Sassen and Moore (1988) in their study of high-rank gas condensates from Upper Jurassic Smackover Formation reservoirs in the southeastern United States. Within any one compound group, as carbon number, or length of side chain, increases with increasing temperature, compound stability decreases. *Thermally stressed saturated hydrocarbons are readily characterized by low or zero concentrations of pristane and phytane.*

These observations regarding the relative thermal stability of the different saturated-hydrocarbon compound classes in the aqueous-pyrolysis experiments require discussion. Firstly, the naphthenes might be expected to undergo aromatization rather than simply to thermally crack, and to a limited extent this may have occurred. However, in the aqueous-pyrolysis experiments for all rocks C_{15}+ aromatic-hydrocarbon concentrations also strongly decreased in going from the maximum of C_{15}+ hydrocarbon generation (333˚C) to hydrocarbon-thermal destruction (350˚C). For example, C_{15}+ aromatic hydrocarbons for the Phosphoria shale decreased from 27.3 mg/g rock at 333˚C to 7.93 mg/g rock at 350˚C. Hence, a wholesale aromatization of naphthenes appears unlikely. Secondly, the observations about the relative thermal stability of the different saturated-hydrocarbon compound classes contradict Mango's (1990) conclusions that the naphthenes are the most stable saturated-hydrocarbon class. Mango's (1990) conclusions and discussion are

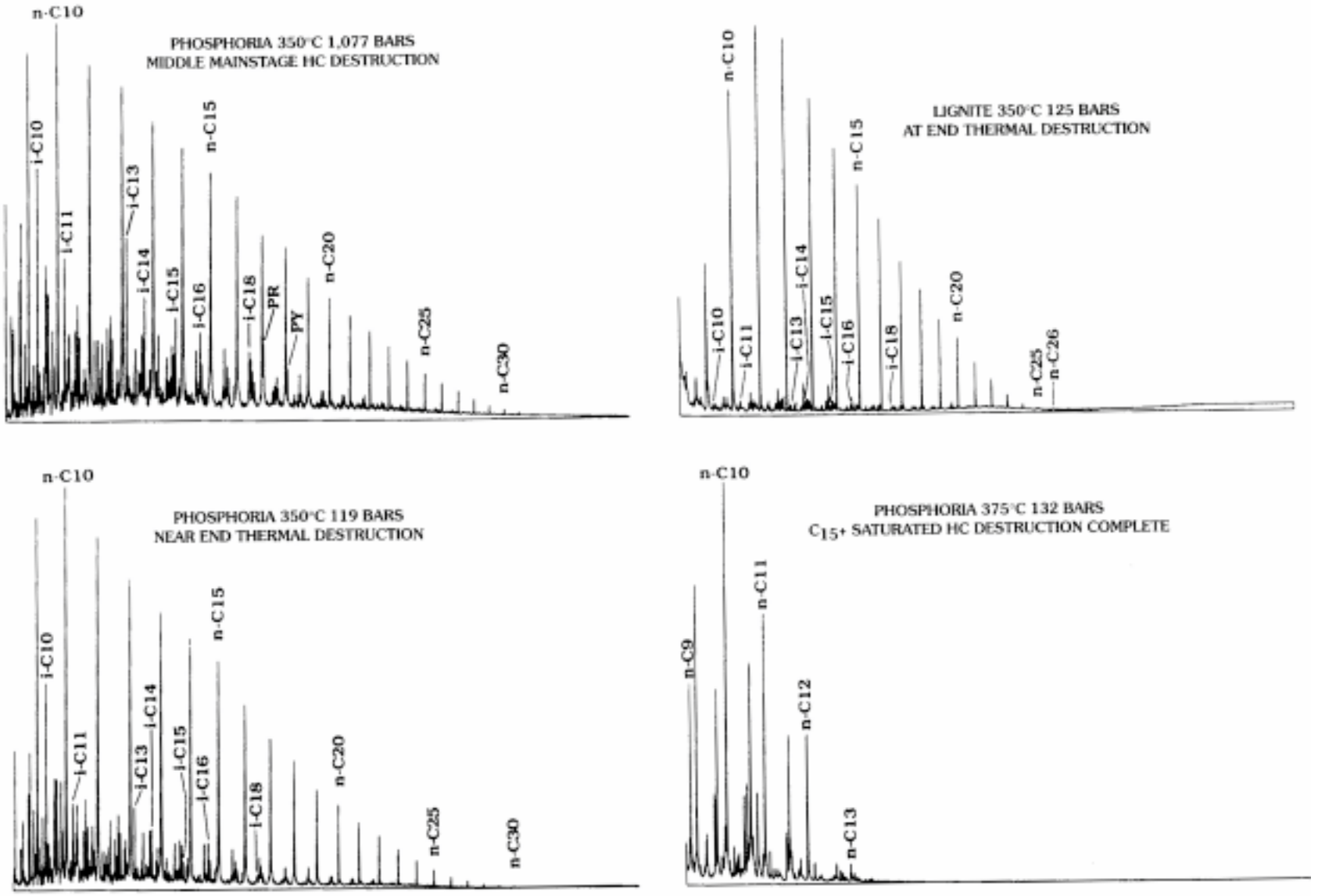

Figure 21. Gas chromatograms of C_8+ saturated hydrocarbons generated by aqueous pyrolysis of the Lower Permian Phosphoria Formation and on a lignite. Compound labeling as in figure 20 caption.

based principally, however, on the C_5–C_9 cyclo-alkanes, and his principal conclusions in this regard are in agreement with other data of this study. Namely, (1) the single ring cyclo-alkanes are remarkably thermally stable, and (2) there is no evidence that the high concentrations of C_5–C_9 cyclo-alkanes in oils are derived from the decomposition of 4- to 5-ringed naphthenes.

Mango (1990) actually provided no conclusive evidence for enhanced thermal stability of 4- to 5- ringed naphthenes. The one multi-ring (bicyclic) compound he discussed, decahydronaphthalene (decalin), is not present in abundance in nature. A thermal cracking experiment he carried out (cholestane and octadecane at 330˚C, dry?, 4 weeks) showed, if anything, that the naphthene was less thermally stable than the n-paraffin (17 versus 2.3 percent destruction, respectively). A more meaningful experiment would, however, be in a wet system at 345˚C–350˚C with cholestane and a higher molecular weight n-paraffin (for example, C_{27}–C_{30}). Furthermore, as is discussed later, natural samples also exhibit greatly reduced concentrations of 4- to 5- ringed naphthenes relative to equivalent carbon-numbered n-paraffins during thermal destruction. Also, as stated, Sassen and Moore (1988) also concluded, in their study of thermally stressed gas condensates, that the n-paraffins are the most stable higher molecular weight species within the saturated hydrocarbons.

C_8+ saturated-hydrocarbon gas chromatograms from highly mature gas condensates from Upper Jurassic Smackover Formation reservoirs in Alabama from the Chatom and Big Escambia Creek fields are shown in figure 22. The marked similarity between these two chromatograms and the C_8+ saturated-hydrocarbon chromatogram from the Phosphoria shale 350˚C, 119-bar experiment (fig. 22) strongly suggests that the two gas condensates were derived from, or exposed to, conditions equivalent to main-stage saturated-hydrocarbon-thermal destruction.

Gas chromatograms of C_{15}+ saturated hydrocarbons (fig. 23) from high-rank rocks of deep wellbores are quite mature. Nonetheless, comparison to the C_{15}+ saturated-hydrocarbon chromatogram from the Phosphoria shale 350˚C, 119-bar experiment suggests that, except for the Foerster–1 sample, none of the other samples has entered main-stage hydrocarbon destruction. Four of these chromatograms (Rogers–1, Lowe–1, and two Jacobs–1), in spite of their extreme maturation ranks, have large pristane and phytane peaks and significant naphthenic envelopes. The reduced pristane and phytane peaks in the chromatogram from the Foerster–1 sample, and other data discussed in Price and Clayton (1990) not discussed here, show that the Foerster–1 sample has just entered C_{15}+ saturated-hydrocarbon-thermal destruction. The apparent large naphthenic envelope of the Foerster–1 sample is an analytical artifact caused by laboratory evaporative loss of C_{18-} hydrocarbons.

Differences between the Foerster–1 and Rogers–1 chromatograms can be ascribed to differences in paleo-fluid

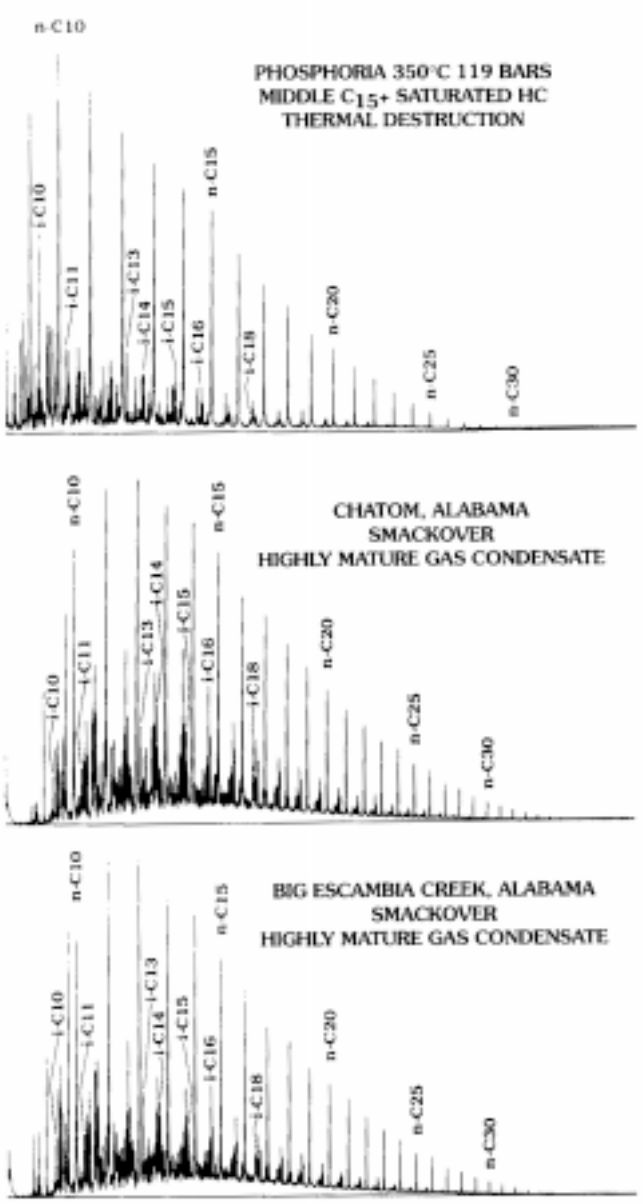

Figure 22. Gas chromatograms of C_8+ saturated hydrocarbons from two highly mature Upper Jurassic Smackover Formation gas condensates from the Chatom and Big Escambia Creek fields, Alabama, and generated by aqueous pyrolysis of shale from the Lower Permian Phosphoria Formation. Compound labeling as in figure 20 caption.

pressures. The deeper Rogers–1 sample has an extrapolated vitrinite reflectance value of 7.6 percent as compared to an extrapolated value of 7.0 percent for the Foerster–1 sample. The saturated hydrocarbons from the Foerster–1 sample have, however, attained slightly higher levels of organic-matter metamorphism than those from the Rogers–1 sample. The 2,750-m-deeper Rogers–1 sample would have experienced substantially (25–50 percent) higher paleo-fluid pressures than the Foerster–1 sample, assuming near lithostatic abnormal fluid pressure gradients at the time of maximum

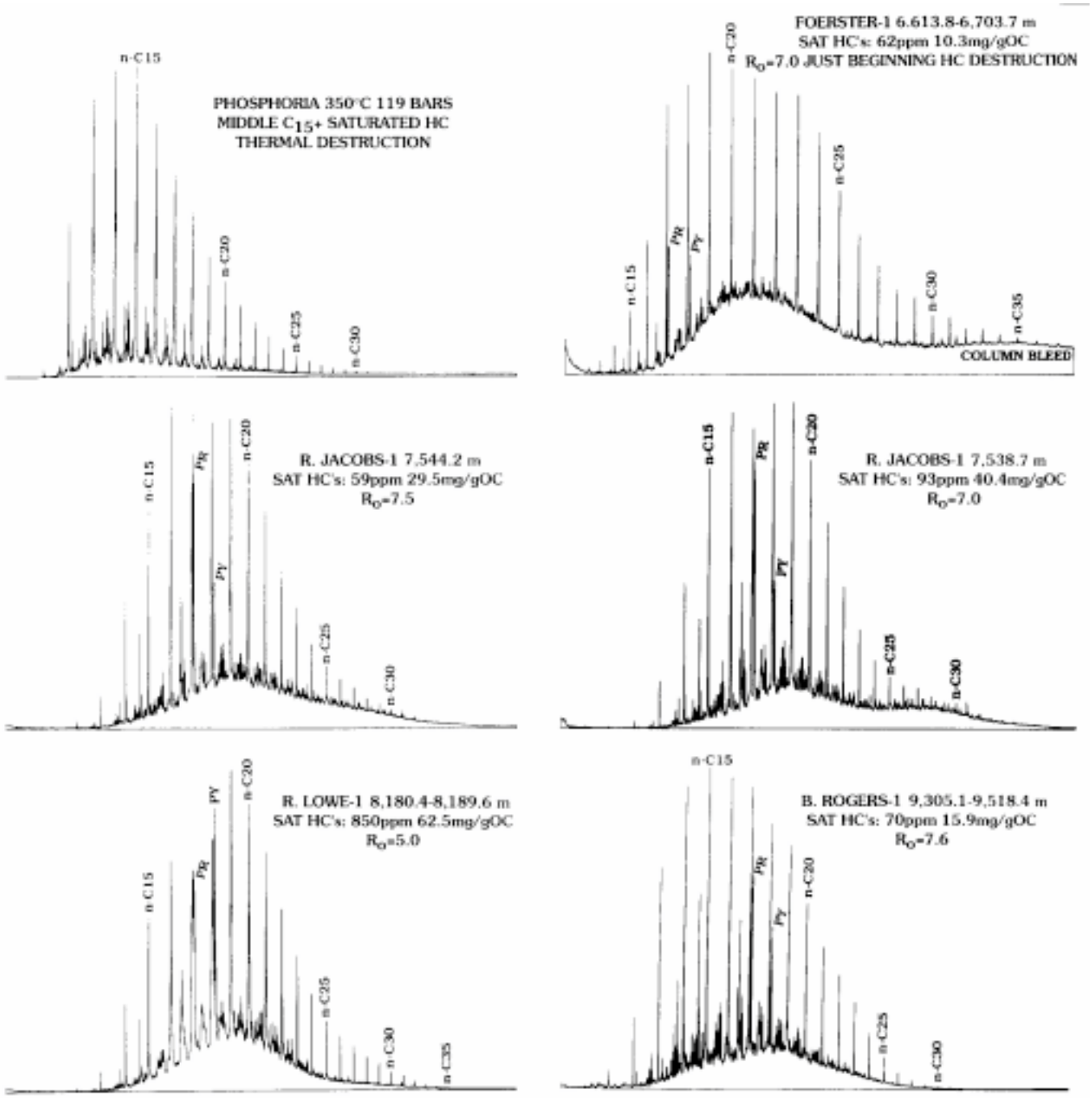

Figure 23. Gas chromatograms of C_{15}+ saturated hydrocarbons from deep rocks of the Rogers–1, Foerster–1, Lowe–1, and Jacobs–1 wellbores (table 1) and generated by aqueous pyrolysis of the Lower Permian Phosphoria Formation. C_{15}+ saturated hydrocarbon concentrations are in parts per million and normalized to rock total organic carbon (mg/gOC), and vitrinite reflectance (R_o) values (extrapolated or read; in percent) are given for each rock sample above the respective chromatogram. Compound labeling as in figure 20 caption.

heat flow for the two wells. Thus, the Foerster–1 sample could have achieved a higher level of organic-matter metamorphism than the Rogers–1 sample because of lower paleo-fluid pressures.

Data from high-rank rocks from deep wellbores demonstrate that C_{15}+ saturated hydrocarbons persist to extrapolated vitrinite reflectance values of about, or above, 7.6 percent in conditions of normal or low paleo-geothermal gradients, and probably to values slightly below 7.0 percent in conditions of very high paleo-geothermal gradients, because of the suppression effect that increasing fluid pressures have on organic-matter metamorphism. Furthermore, high concentrations of bitumen and C_{15}+ hydrocarbons (fig. 17) can persist to reflectances of 3.0–5.0 percent.

These conclusions relate, however, only to the high-rank persistence of hydrocarbons in highly pressurized, fine-grained rocks (closed-chemical systems) that do not allow product escape. These conclusions have no bearing on either hydrocarbon-generation reactions, which occur at much lower ranks, or on the possible existence of commercial-oil deposits at high maturation ranks.

COMPOSITIONAL CHANGES IN AROMATIC HYDROCARBONS DURING DESTRUCTION

Aromatic hydrocarbons, similar to saturated hydrocarbons, compositionally evolve through main-stage hydrocarbon generation as demonstrated by C_8+ aromatic-hydrocarbon gas chromatograms from aqueous-pyrolysis experiments on the Anna Shale (fig. 24). The chromatogram of the immature sample is dominated by one large peak (which elutes in the range of the alkylated benzenes) and has an unresolved naphtheno-aromatic hump on which there are few peaks of significant size. The chromatogram from the sample at commencement of hydrocarbon generation (250˚C) has significant differences, in particular, a series of well-defined peaks on a large naphtheno-aromatic hump. Aromatic hydrocarbons from mature (333˚C) samples (1) are biased toward lighter compounds, (2) have a greatly reduced unresolved (naphtheno-aromatic) hump, (3) have reduced-peak heights of higher molecular weight aromatic hydrocarbons, (4) are characterized by large concentrations of alkylated benzenes, alkylated naphthalenes, and alkylated phenanthrenes, (5) and have alkylated benzo- and dibenzothiophenes as the principal sulfur-bearing aromatic compounds.

Throughout hydrocarbon-thermal destruction, the aromatic hydrocarbons are both more complex and thermally stable than the saturated hydrocarbons, as shown by C_8+ aromatic-hydrocarbon gas chromatograms from aqueous-pyrolysis experiments on the Phosphoria shale (fig. 25). In these experiments, C_8+ aromatic hydrocarbon concentrations decreased from a maximum value of 33.8 mg/g rock at the maximum of hydrocarbon generation (333˚C, 80.8 bars) to 11.7 mg/g rock in the middle of main-stage hydrocarbon-thermal destruction (350˚C, 119 bars). In the 350˚C, 119-bar chromatogram, the unresolved naphtheno-aromatic hump is small, and the chromatogram is dominated by large peaks of alkylated: benzenes, naphthalenes, benzothiophenes, dibenzothiophenes, and phenanthrenes. In the 375˚C, 132-bar experiment, C_{15}+ saturated hydrocarbons were thermally destroyed (fig. 21); however, a suite of C_{15}+ aromatic hydrocarbons persists both in this experiment and in the 400˚C, 144-bar experiment. These experimental data demonstrate that aromatic hydrocarbons are much more thermally stable than saturated hydrocarbons. The 375˚C, 132-bar chromatogram of figure 25 is simpler than that of the 350˚C, 119-bar experiment, in part because of the

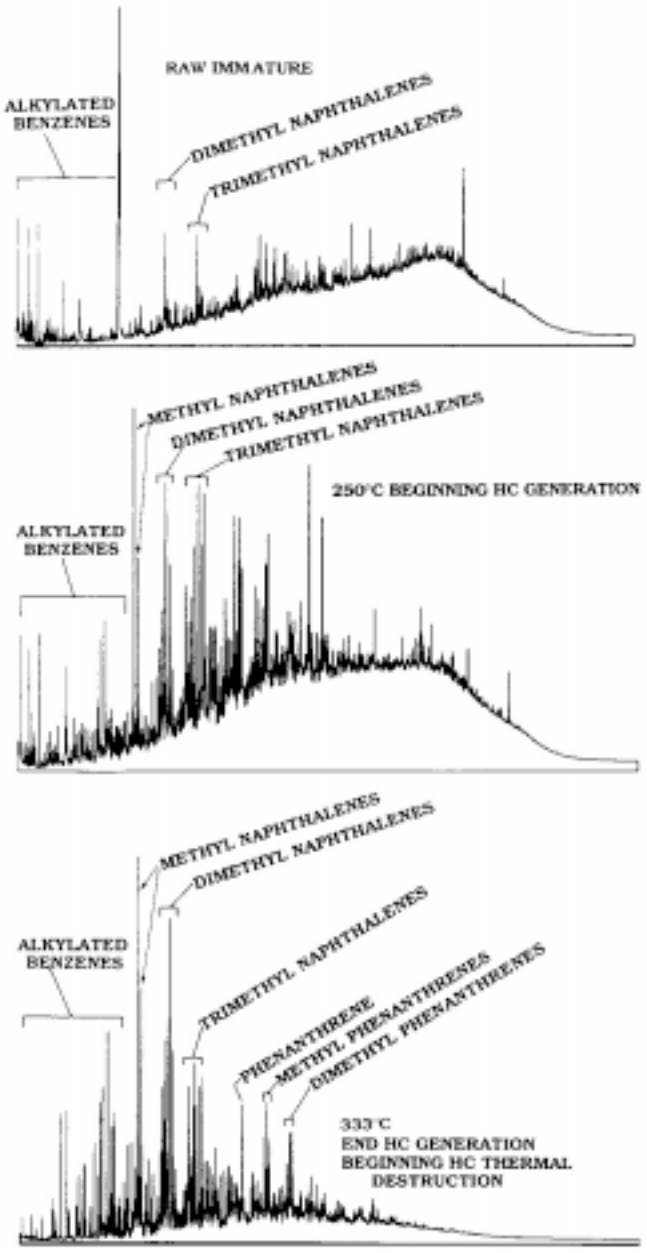

Figure 24. Gas chromatograms of C_8+ aromatic hydrocarbon generated by aqueous pyrolysis of carbonaceous shale from the Middle Pennsylvanian Anna Shale Member and from the unreacted (immature, vitrinite reflectance=0.25 percent) rock.

thermal destruction of the methylated benzothiophenes whose peaks no longer interfere with those of the methylated naphthalenes. The aromatic hump has also completely disappeared in the 375˚C sample. The 400˚C, 144-bar experiment (fig. 25) is equivalent to conditions of true rock metamorphism, yet a moderately complex distribution of aromatic hydrocarbons persists even under these conditions. In the 400˚C experiment, aromatic hydrocarbons are dominated by both (1) parent compounds (for example, naphthalene, fluorene, phenanthrene, and dibenzothiophene) and (2)

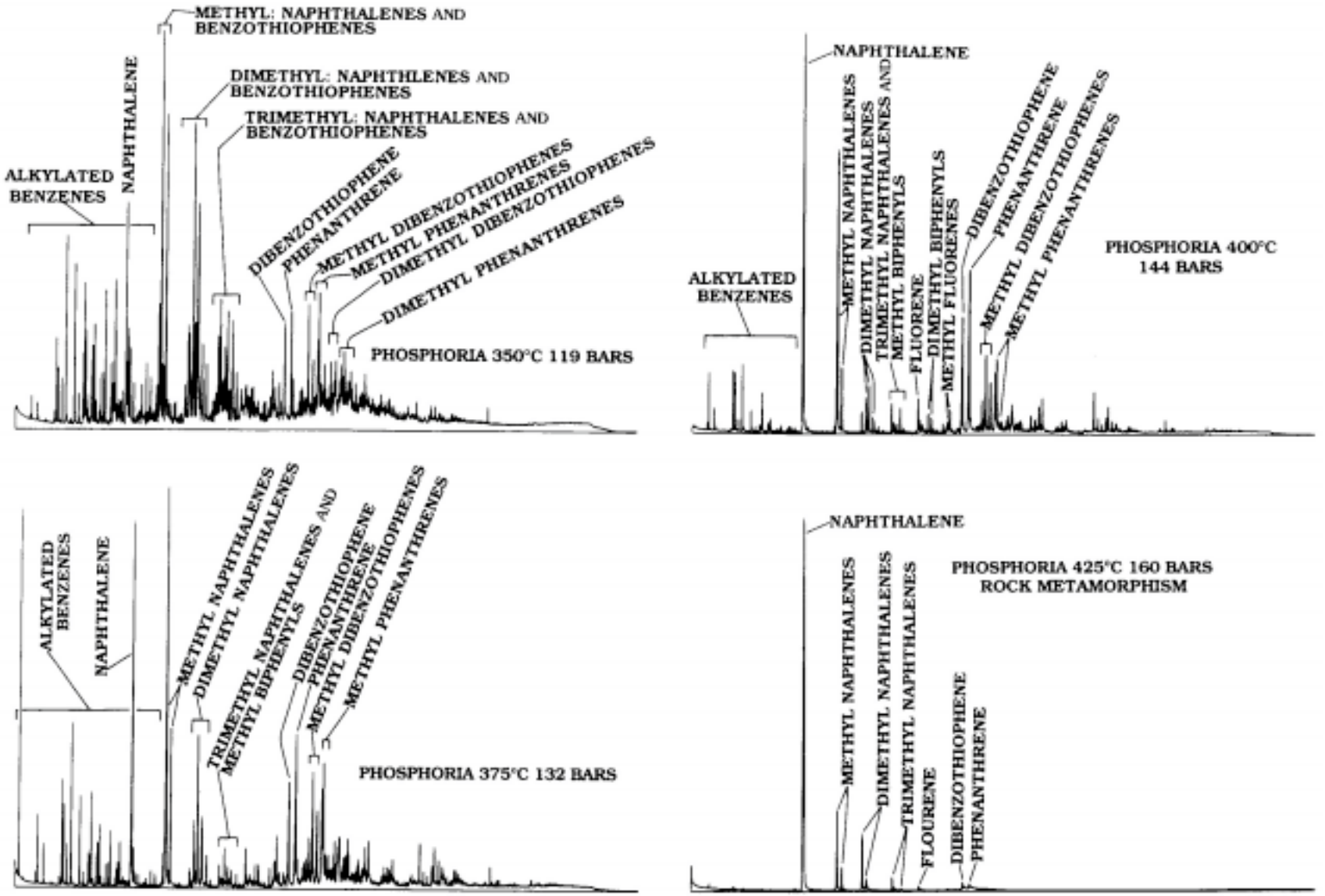

Figure 25. Gas chromatograms of C_8+ aromatic hydrocarbons generated by aqueous pyrolysis of shale from the Lower Permian Phosphoria Formation in experiments that were in the hydrocarbon thermal destructive phase.

Table 5. Normalized percentages for aromatic hydrocarbon compound classes eluting between the dimethylbenzenes and the trimethylnaphthalenes, as determined by full-scan mass spectrometry, for aqueous-pyrolysis experiments on shale from the Phosphoria Formation (Lower Permian).

[Each vertical column of normalized percentages sums to 100 percent±1 percent. Number in parentheses after compound class is approximate molecular weight. Temperature and pressure represent experimental conditions. Last line is the total of the C8+ aromatic hydrocarbons determined for each experimental run by a combination of gas chromatography and gravimetrics, on an analytical balance, in milligrams of hydrocarbons per gram of reacted rock. Mass spectrometry, being very sensitive, determines the presence of compounds not recognized by gravimetrics. ND indicates not determined]

	Normalized percentages								
Compound class	Temperature Pressure	500°C 226.5 bars	450°C 192 bars	425°C 160 bars	425°C 551 bars	440°C 144 bars	375°C 132 bars	350°C 118 bars	350°C 1,077 bars	333°C 80.8 bars
Dimethylbenzenes (106)		0.68	0.83	2.31	8.39	7.81	12.50	4.80	1.12	0.81
Alkylated benzenes (120)		0	0.15	0.58	4.70	4.75	7.02	19.41	24.14	1.06
Alkylated benzenes (134)		0	0.02	0.02	0.30	0.46	1.87	3.59	3.62	0.28
Alkylated benzenes (148)		0	0	0	0.01	0.03	0.23	1.43	2.49	0.34
Alkylated benzenes (162)		0	0	0	0	0.003	0.03	0.42	0.69	0.08
Alkylated benzenes (176)		0	0	0	0	0	0	0.10	0.85	0.06
Alkylated benzenes (190)		0	0	0	0	0	0	0	0.07	0.05
Naphthalene (128)		28.55	77.79	87.08	70.43	62.37	48.02	8.56	1.78	0.41
Methylnaphthalene (142)		0.18	1.49	5.94	13.94	22.12	23.00	22.91	20.33	10.82
Dimethylnaphthalene (156)		0	0.17	0.14	0.50	1.14	4.10	11.12	11.02	11.36
Trimethylnaphthalene (170)		0	0	0.04	0.57	0.03	0.76	5.83	6.97	15.80
Biphenyl (154)		70.14	19.46	3.75	0.33	0.03	0.02	0.03	0.02	0.07
Methylbiphenyl (168)		0.45	0.07	0.86	0.86	0.41	0.27	0.36	0.11	0.54
Benzofuran (118)		0	0.01	0.04	0.20	0.04	0.04	0.05	0.11	0.01
Methylbenzofuran 132)		0	0.02	0.01	0.11	0.30	0.35	1.79	1.11	0.31
Dimethylbenzothiophene (146)		0	0	0	0.10	0.01	0.08	0.37	1.44	0.21
Trimethylbenzofuran (160)		0	0	0	0	0	0.02	0.24	0.53	0.24
Benzothiophene (134)		0	0.01	0.003	0.01	0.06	0.30	1.17	0.27	0.44
Methylbenzothiophene (148)		0	0	0	0.01	0.08	0.71	6.16	5.64	15.35
Dimethylbenzothiophene (162)		0	0	0	0.01	0.05	0.61	8.14	7.76	16.25
Trimethylbenzothiophene (176)		0	0	0	0	0.01	0.05	3.53	10.89	25.11
Alkylated thiophene (112)		0	0	0	0	0	0	0.01	0.01	0.04
Alkylated thiophene (126)		0	0	0	0	0	0	0	0.24	0.07
Alkylated thiophene (140)		0	0	0	0	0	0	0	0.24	0.23
Alkylated thiophene (154)		0	0	0	0	0	0	0	0.03	0.01
Alkylated thiophene (168)		0	0	0	0	0	0	0	0.004	0
Alkylated thiophene (182)		0	0	0	0	0	0	0	0	0
Alkylated thiophene (196)		0	0	0	0	0	0	0	0	0
Alkylated thiophene (210)		0	0	0	0	0	0	0	0	0
C8+ aromatic hydrocarbons		ND	2.214	6.22	6.76	6.37	7.02	11.70	23.06	33.78

methyl variants of the parent compounds. Furthermore, dimethyl- and trimethyl-variants are in reduced concentrations, and more highly alkylated species have been destroyed (fig. 25, tables 5, 6).

Several points of qualification should be discussed. First, the aqueous-pyrolysis data of figure 25 and tables 5 and 6 are for aromatic hydrocarbons generated by the very sulfur rich organic matter of the Retort Member of the Phosphoria Formation. The organic matter in almost all other rocks in nature contains far less sulfur and therefore generates far lower quantities of sulfur-bearing aromatic hydrocarbons. The high concentrations of sulfur-bearing aromatic hydrocarbons in figure 25 and tables 5 and 6 are also present in lower temperature aqueous-pyrolysis experiments on the Phosphoria shale. As such, pure aromatic-hydrocarbon peaks (for example, the naphthalenes) are in smaller concentrations and even in some experiments dwarfed by the sulfur-bearing aromatic hydrocarbons. Although sulfur-rich organic matter is present in nature, it is not the norm. Thus, the high-rank aromatic-hydrocarbon compositions of the Phosphoria shale (fig. 25) should not be considered representative. For example, for organic matter having lower sulfur contents, the high concentrations of the alkylated benzothiophenes would be lower at experimental temperatures lower than 375˚C (table 5), and the high concentrations of dibenzothiophene and the methyldibenzothiophenes would be lower at all experimental temperatures (table 6).

A second point to consider is that with high concentrations of sulfur-bearing aromatic hydrocarbons the utility of gas chromatography as an analytical tool is greatly diminished. This is because sulfur-bearing aromatic hydrocarbons coelute with the “normal” aromatic hydrocarbons

Table 6. Normalized percentages for aromatic hydrocarbon compound classes eluting roughly between the trimethylnaphthalenes and the methylphenanthrenes, as determined by full-scan mass spectrometry, for aqueous-pyrolysis experiments on shale from the Phosphoria Formation (Lower Permian).

[Each vertical column of normalized percentages sums to 100 percent±1 percent. Number in parentheses after compound class is approximate molecular weight. Temperature and pressure represent experimental conditions]

	Normalized percentages								
Compound class	Temperature Pressure	500°C 226.5 bars	450°C 192 bars	425°C 160 bars	425°C 551 bars	440°C 144 bars	375°C 132 bars	350°C 118 bars	350°C 1,077 bars	333°C 80.8 bars
Trimethylnaphthalenes (170)		0	0.05?	0	0.02	0.03	0.23	12.88	24.06	20.70
Tetramethylnaphthalenes (184)		0	0	0	0.03	0.10	0.95	8.82	11.68	15.75
Pentamethylnaphthalenes (198)		0	0	0	0	0.01	0.08	3.09	8.72	5.60
Fluorene (166)		25.62	2.80	2.25	0.64	0.56	0.69	2.45	0.068	0.13
Methylfluorenes (180)		0	0.16	0.16	0.20	0.35	1.45	1.38	0.45	0.50
Dimethylfluorenes (194)		0	0	0.02	0.06	0.16	1.19	1.91	1.04	0.86
Dibenzothiophene (184)		10.89	69.52	42.14	36.43	31.18	25.29	8.96	3.63	4.61
Methyldibenzothiophenes and methylnapthobenzothiophenes (198)		0	0.18	1.87	7.62	8.99	17.94	24.01	21.32	22.58
Methylbiphenyl (182)		0	0.03	0.26	0.19	0.74	1.35	1.35	0.87	1.18
Dimethylbiphenyls (196)		0	0	0.02	0.23	0.55	1.24	1.67	1.87	2.02
Phenanthrene (178)		63.49	26.84	52.45	47.43	47.64	31.42	9.09	1.10	1.19
Methylphenanthrenes (192)		0	0.13	0.79	6.11	0.86	17.19	19.71	8.835	6.14
Methyldibenzofurans (182)		0	0.08	0.04	0.26	0.23	0.49	1.36	1.52	2.21
Dimethyldibenzofurans (196)		0	0.08	0.01	0.08	0.17	0.28	1.12	1.58	2.52
Trimethylbenzothiophenes (176)		0	0	0	0	TR	0	1.52	2.74	2.80
Tetramethylbenzothiophenes (190)		0	0	0	0	0	0	1.83	9.49	9.93
Methylacenaphthenes (166)		0	0.13	0.02	0.70	0.10	0.19	1.03	0.95	1.26
Alkylbenzenes (106–190)		0	0	0	0	0	0	0.03	0.08	TR

beginning with the methyldibenzothiophenes coeluting with the methylnaphthalenes and proceeding through the methyldibenzothiophenes coeluting with the methylphenanthrenes. Thus, quantitative, and even qualitative, gas chromatography is impossible with the aromatic hydrocarbons from samples containing sulfur-rich organic matter, such as those from the aqueous-pyrolysis experiments on the Phosphoria shale, and mass spectrometry is necessary. Also, flame-ionization detection gas chromatography mostly measures carbon-hydrogen bonds. Thus, the same concentration of a highly alkylated species gives a much higher response than an equal weight of the parent compound; for example, pentamethylnaphthalene gives a much higher response than naphthalene in equal concentrations. Therefore, overall, mass spectrometry is a better analytical tool for aromatic hydrocarbon analyses than gas chromatography.

The data of tables 5 and 6 (and fig. 25) demonstrate that unusual suites of aromatic-hydrocarbon distributions are present in experiments even beyond 400˚C. These data strongly suggest that low concentrations of such simple aromatic hydrocarbon distributions (1) should extend well into some high-pressure, high-temperature rock-metamorphic facies, (2) should be present in inclusions in some of the minerals of these regimes, and (3) may be utilitarian as geothermic-geobaric research tools.

The aqueous-pyrolysis experiments of Wenger and Price (1991) and Price and Wenger (1991) show that, irrespective of the starting organic-matter type, in the thermal-destructive phase, repetitive exact, or very similar, aromatic-hydrocarbon distributions result, no doubt from response to thermodynamic and kinetic dictums on the systems. Such aromatic-hydrocarbon distributions should be present and observable from many different high-pressure, high-temperature geologic regimes, including high-rank deeply buried sedimentary rocks. An example of very similar aromatic-hydrocarbon distributions is given in figure 26 for aqueous-pyrolysis experiments performed in the C_{15}+ hydrocarbon thermal-destructive phase on rocks containing different organic-matter types (table 1): a Los Angeles Basin mid-Miocene shale (type II/III) and the Eocene shale of the Green River Formation (type I). In spite of the large differences in organic-matter type, the two sets of chromatograms are very similar. The 350˚C chromatograms (1) are dominated by the methyl-, dimethyl-, and trimethylnaphthalenes and the methyl- and dimethylphenanthrenes, (2) have reduced naphtheno-aromatic unresolved envelopes (humps), and (3) have a pronounced absence of higher molecular weight compounds that are present in lower rank samples (for example, fig. 24, Anna Shale, 250˚C and 333˚C samples). The 375˚C chromatograms (fig. 26) (1) have essentially no unresolved hump, (2) have increased concentrations of methylated-naphthalenes relative to methylated-phenanthrenes, and (3) are simpler in that they have a significantly reduced number of prominent peaks.

The same, or very similar, aromatic-hydrocarbon distributions present in high-temperature aqueous-pyrolysis

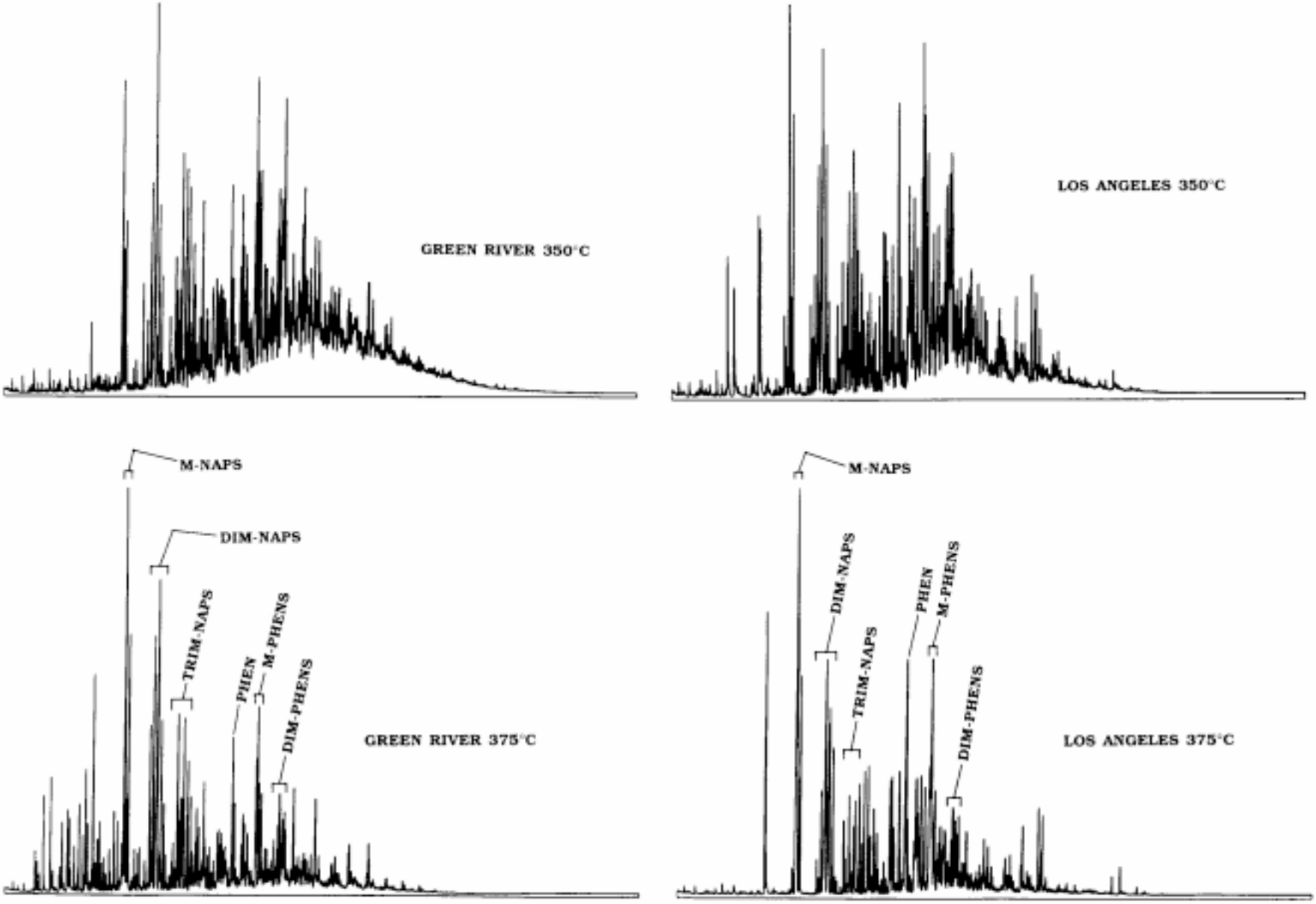

Figure 26. Gas chromatograms of C_8+ aromatic hydrocarbons generated by aqueous pyrolysis of shale from the Eocene Green River Formation and from the Los Angeles Basin, California (mid-Miocene). M-NAPS, methyl-naphthalenes; DM-NAPS, dimethyl-naphthalenes; TRIM-NAPS, trimethylnaphthalenes; PHEN, phenanthrene; M-PHENS, methyl-phenanthrenes; DIM-PHENS, dimethyl-phenanthrenes.

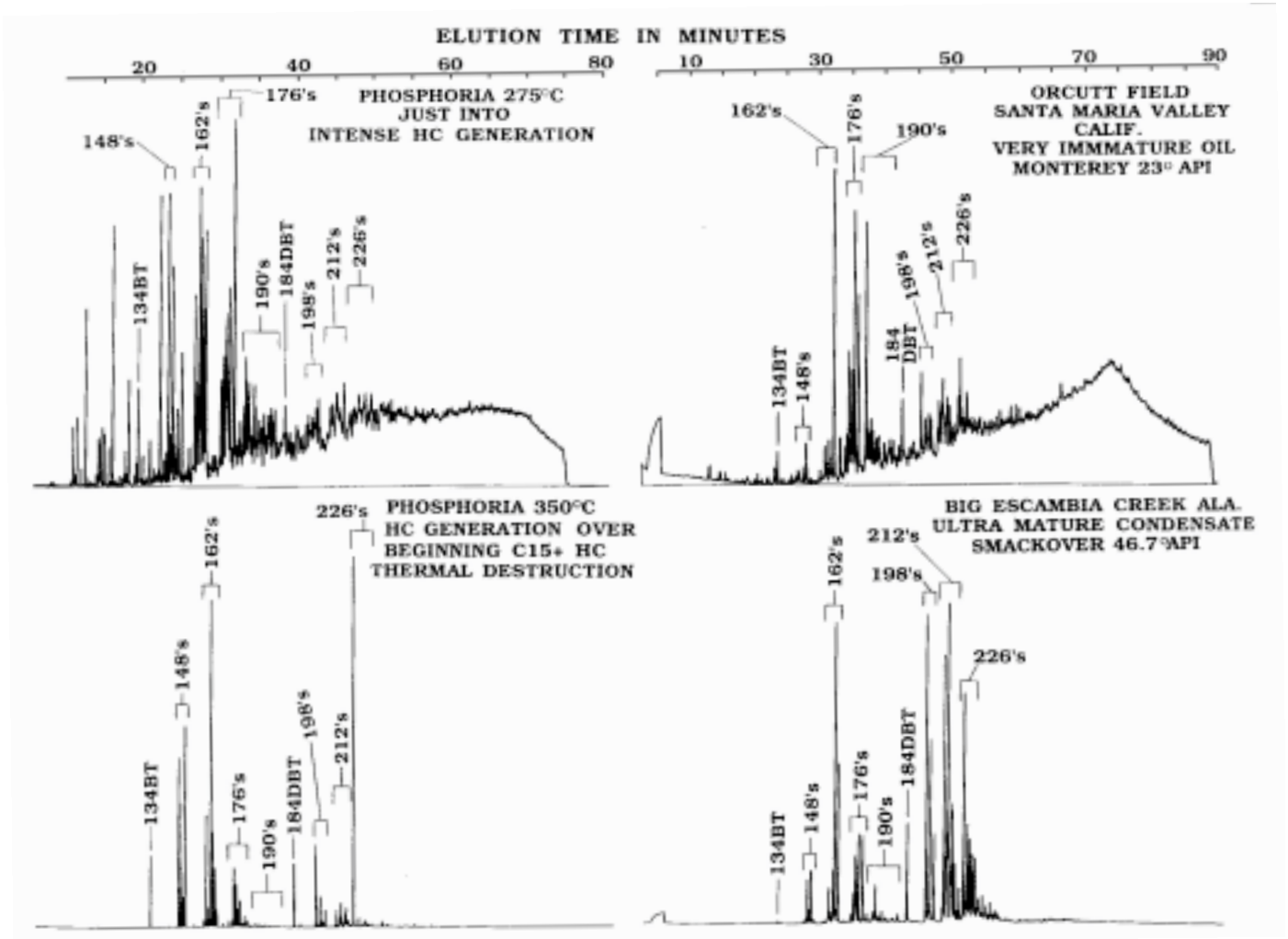

Figure 27. C_8+ (flame-photometric detection) gas chromatograms of sulfur-bearing aromatic hydrocarbons from an immature oil from the Orcutt field, Santa Maria Valley, California, Miocene Monterey Formation (0.916 g/cm^3 specific gravity); from a mature gas-condensate from the Big Escambia Creek field, Escambia County, Alabama, Upper Jurassic Smackover Formation (0.794 g/cm^3 specific gravity); and generated by two aqueous-pyrolysis experiments performed on shale from the Lower Permian Phosphoria Formation that is comparable in maturity to the oil and gas condensate samples. Unlabeled peaks in the front third of the Orcutt field and Lower Permian Phosphoria 275˚C chromatograms are series of alkylated thiophenes. Numbers (and letters) above the peaks refer to molecular weights and compound classes: 134BT, benzothiophene; 148's, methylbenzothiophenes; 162's, dimethylbenzothiophenes; 176's, trimethylbenzothiophenes; 190's, tetramethylbenzothiophenes; 184BT, dibenzothiophene; 198's, methyldibenzothiophenes; 212's, dimethyldibenzothiophenes; 226's, trimethyldibenzothiophenes.

experiments (333˚C–375˚C) are also present in high-rank natural samples. For example, flame-photometric detection (specific for sulfur-bearing compounds) gas chromatograms are shown for C_8+ aromatic-hydrocarbon fractions from two natural samples and from two samples from aqueous-pyrolysis experiments of equivalent maturities (fig. 27). The Phosphoria 275˚C and Orcutt oil field samples (1) are both immature, (2) have large unresolved humps, and (3) have significant concentrations of alkylated-thiopenes (molecular weights 112, 126, 140, 154, 168, 182, 196, 210, and so on; not labeled in fig. 27 but range from the first eluting peaks to about dibenzothiophene –184 DBT). The Phosphoria 350˚C and Big Escambia Creek field Phosphoria samples (1) are highly mature, (2) have no alkylated thiophenes, which were thermally destroyed at lower ranks (only traces of 112–154 molecular weight alkylated thiophenes persist to 333˚C, and no 168+ molecular weight thiophenes persist past 333˚C in the aqueous-pyrolysis experiments, table 5), and (3) are much simpler in that the methyl-, dimethyl-, and trimethylbenzothiophenes and dibenzothiophenes make up almost all of the sulfur-bearing aromatic hydrocarbons.

Details of changes within the higher molecular weight (methyldibenzo-thiophenes and heavier compounds) sulfur-bearing aromatic hydrocarbons as a function of maturity are shown in the flame-photometric detection gas chromatograms of figure 28 for three natural samples and for three aqueous-pyrolysis samples of equivalent maturities. The Cottonwood Creek oil sample and Phosphoria 287˚C sample

are both moderately mature; large unresolved envelopes of high-molecular compounds make up most of the samples, and only a limited number of well-resolved peaks are on top of this envelope. The "M-DBT's" peaks in both samples are made up by the 1-, 2-, 3- and 4-methyldibenzothiophenes and by a yet unidentified series of methylnaphthothiophenes; the latter group of compounds are in higher concentrations in the Phosphoria sample. Dimethyl-, trimethyl-, and tetramethyl-naphthothiophenes also coelute with the respective different classes of alkylated-dibenzothiophenes. The Pollard oil and 333˚C Phosphoria samples (1) are mature and (2) have greatly reduced unresolved envelopes, and (3) the methyl-, dimethyl-, and trimethyl-dibenzothiophenes and naphthothiophenes (198, 212, and 226 molecular weight compounds) make up a significant percentage of each sample. No obvious alkylated-naphthothiophenes are present in the Pollard sample; this may be due, however, more to facies control of the original organic matter from which the Pollard oil was derived than to a maturity control. The Phosphoria 375˚C and Flomaton samples (1) are ultramature and well into the C_{15}+ hydrocarbon-thermal destructive phase, (2) have no unresolved hump of higher molecular-weight sulfur-bearing aromatic hydrocarbons, and (3) are made up almost entirely of the (198) methyl-, (212) dimethyl-, and (226) trimethyldibenzothiophenes. A series of higher molecular weight compounds (possibly naphthobenzothiophenes?) is present in higher concentrations in the Phosphoria 375˚C sample as compared to the Flomaton sample. Note the similar distribution of methyl-, and dimethyl-dibenzothiophenes in both samples.

C_{15}+ non-sulfur-bearing aromatic-hydrocarbon distributions from deeply buried high-rank rocks from nature show the same trends as in aqueous-pyrolysis experiments at equivalent ranks as C_{15}+ hydrocarbon-thermal destruction is approached (fig. 29). Because of its rank (R_o=0.97 percent), the Ralph Lowe 2,709.5–2,712.6-m sample would be considered mature by many petroleum geochemists; however, its aromatic-hydrocarbon chromatogram is far less mature than the other chromatograms of figure 29. Among other characteristics, the Ralph Lowe chromatogram (1) has a pronounced unresolved hump that extends to high-molecular-weight compounds and (2) has a significant percentage of higher molecular weight compounds. The 8,210.9–8,357.2-m (R_o=4.8 percent) Bertha Rogers C_{15}+ aromatic-hydrocarbon gas chromatogram has a reduced unresolved envelope, significantly reduced concentrations of higher molecular weight compounds, and a bias towards methyl-, dimethyl-, and trimethylnaphthalenes and phenanthrenes. These trends strengthen through the Bertha Rogers 9,125.3–9,189.3-m (R_o=6.9 percent) and 9,305.1–9,518.4-m (R_o=7.4 percent) samples. As discussed above, C_{15}+ hydrocarbon-thermal destruction was probably suppressed in the deep Bertha Rogers samples by high fluid pressures (2,150 bars or greater?) most likely present in the rocks at the time of maximum paleo-heat flow in the basin. Thus, even though the hydrocarbons of the deeper rocks in this well are at R_o=7.0 percent, they have not yet begun C_{15}+ hydrocarbon-thermal destruction. The deepest samples from the Foerster–1 wellbore were, however, at lower fluid pressures that apparently allowed C_{15}+ hydrocarbon-thermal destruction to commence in the Foerster–1 at equivalent ranks. Thus, the 6,613.8–6,703.7-m (R_o=7.0 percent) Foerster–1 samples (fig. 29) (1) are mostly made up of methyl-, dimethyl-, and trimethylnaphthalenes, (2) have moderate concentrations of phenanthrene and the methyl- and dimethylphenanthrenes, (3) have very small unresolved envelopes, and (4) have only small concentrations of higher molecular weight compounds. These compositional changes are the same as those observed in the aqueous-pyrolysis experiments in the approach to, and in, C_{15}+ hydrocarbon-thermal destruction (figs. 24–26, tables 5, 6). For example, note that C_{15}+ aromatic-hydrocarbon gas chromatograms for the two deepest Rogers–1 samples (fig. 29) resemble the 350˚C chromatograms of figure 26, whereas chromatograms for the two Foerster–1 have characteristics intermediate between those of the 350˚ and 375˚C chromatograms of figure 26.

The above discussion demonstrates that, similar to saturated hydrocarbons, during C_{15}+ hydrocarbon-thermal destruction the aromatic hydrocarbons follow distinct compositional trends. For example, at high ranks, sulfur-bearing aromatic hydrocarbons are made up principally of the methyl-, dimethyl-, and trimethyl-benzothiophenes and dibenzothiophenes and the parent compounds, benzothiophene and dibenzothiophene (figs. 27, 28). The lower molecular weight thiophenes, and the higher molecular weight sulfur-bearing compounds making up the unresolved hump in gas chromatograms of more immature samples, are all thermally destroyed at high ranks. Non-sulfur-bearing aromatic hydrocarbons at high maturities are made up mostly of the methyl-, dimethyl-, and trimethyl-naphthalenes and phenanthrenes and of the parent compounds naphthalene and phenanthrene. Similar to saturated hydrocarbons, within any one compound group (for example, the naphthalenes), as molecular weight or length of side chain increases, thermal stability greatly decreases. Thus, during C_{15}+ hydrocarbon-thermal destruction, ethyl, propyl, butyl, and so forth side chains are unstable compared to methyl groups. Also, during C_{15}+ hydrocarbon-thermal destruction, all naphtheno-aromatic hydrocarbons are destroyed because of the relative thermal instability of the saturated hydrocarbons that results in the disappearance of the aromatic hump at elevated maturation ranks. Thermally stressed aromatic hydrocarbons are characterized by (fig. 30) (1) high concentrations of alkylated benzenes (especially in oils and condensates), (2) an absence of alkylated thiophenes, (3) high concentrations of methyl-, dimethyl-, and trimethyl-naphthalenes, benzothiophenes, phenanthrenes, and dibenzothiophenes, (4) a small or no unresolved hump, (5) a lack of higher molecular weight compounds, and (6) relatively simple peak distributions.

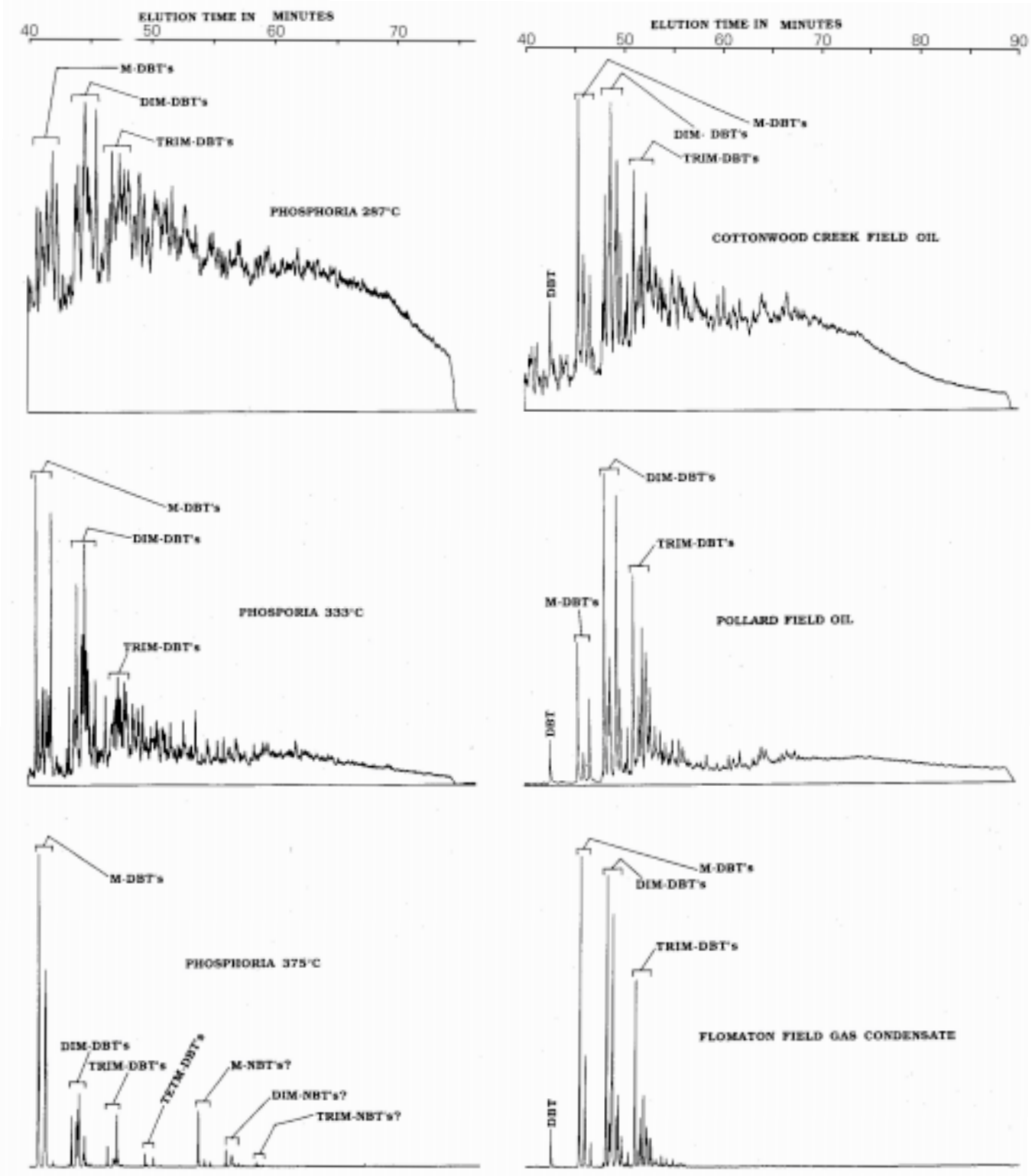

Figure 28. Flame-photometric-detection gas chromatograms of high-molecular-weight sulfur-bearing aromatic hydrocarbons (roughly dibenzothiophene and higher eluting hydrocarbons) generated by three aqueous-pyrolysis experiments on shale from the Lower Permian Phosphoria shale and for two oils and one gas condensate of equivalent maturity to the shale. The Cottonwood Creek oil, Big Horn Basin, Washakie County, Wyoming, is produced from the Phosphoria Formation. The Pollard oil, Escambia County, Alabama, is produced from the Upper Cretaceous Tuscaloosa Formation. The Flomaton gas condensate, Escambia County, Alabama, is produced from the Upper Jurassic Norphlet Formation.

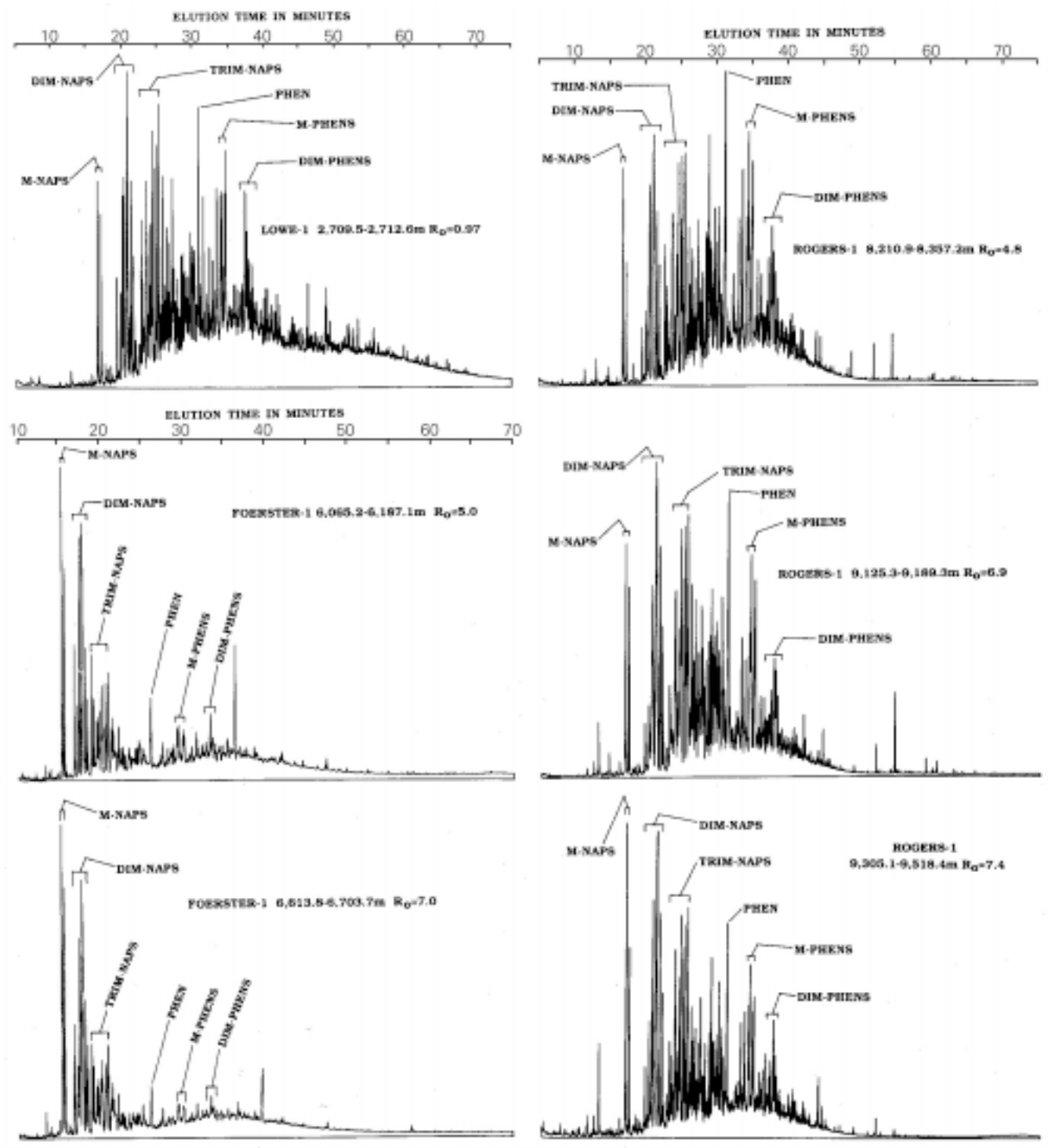

Figure 29. Gas chromatograms of C_{15}+ aromatic hydrocarbon from bitumen extracted from deep rocks of the Bertha Rogers–1, Ralph Lowe–1, and Foerster–1 deep wellbores (table 1). Sample depth and measured, or interpolated, or extrapolated vitrinite reflectance (R_o, in percent) values are given for each chromatogram. M-NAPS, methyl-naphthalenes; DIM-NAPS, dimethyl-naphthalenes; TRIM-NAPS, trimethyl-naphthalenes; PHEN, phenanthrene; M-PHENS, methyl-phenanthrenes; DIM-PHENS, dimethyl-phenanthrenes, and DIM-PHENS are dimethyl-phenanthrenes. The Rogers–1 and Lowe–1 samples were analyzed under the same gas chromatographic conditions, which were different than those used for the Foerster–1 samples.

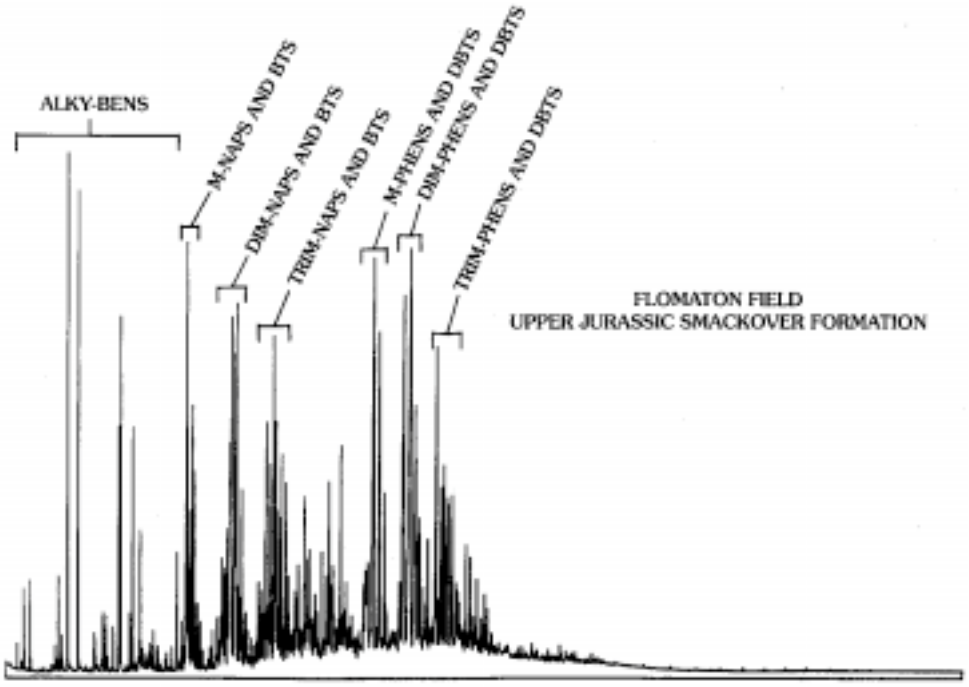

Figure 30. Gas chromatogram (flame-ionization detection) of C_8+ aromatic hydrocarbons of the Flomaton field gas condensate, Escambia County, Alabama, produced from the Upper Jurassic Norphlet Formation. ALKY-BENS, alkylated-benzenes; M-NAPS & BTS, methyl-naphthalenes and methyl-benzothiophenes; DIM-NAPS & BTS, dimethyl-naphthalenes and dimethyl-benzothiophenes; TRIM-NAPS & BTS, trimethyl-naphthalenes and trimethyl-benzothiophenes; M-PHENS & DBTS, methyl-phenanthrenes and methyl-dibenzothiophenes; DIM-PHENS & DBTS, dimethyl-phenanthrenes and dimethyl-dibenzothiophenes; TRIM-PHENS & DBTS, trimethyl-phenanthrenes and trimethyl-dibenzothiophenes.

C_{15}+ HYDROCARBON THERMAL STABILITY—DISCUSSION

Although the hypothesis of thermal instability of C_{15}+ hydrocarbons at moderate burial temperatures (150˚C–200˚C) is generally accepted as a law in petroleum geochemistry, some investigators have questioned the validity of this hypothesis. Shock (1990), Mango (1991), and Helgeson (1991) addressed hydrocarbon thermal stability from theoretical considerations and concluded that hydrocarbons have significantly greater thermal stability than is suggested by current petroleum-geochemical paradigms. Hayes (1991) pointed out that current petroleum-geochemical paradigms regarding C_{15}+ hydrocarbon thermal stability require serious reconsideration.

The above theoretical considerations are supported by the very high activation energies that must be overcome for carbon-carbon bonds to break during hydrocarbon-thermal destruction. The average activation energy for carbon-carbon bond breakage in saturated hydrocarbons is 82.6 kcal/mole (Cottrell, 1958; Pauling, 1960; Eggers and others, 1964; Klotz, 1964; Roberts and Caserio, 1964). The activation energy for carbon-carbon bond breakage of the benzene ring is 117 kcal/mole (Gould, 1959). These differences in bond strengths between saturated and aromatic hydrocarbons explain the much greater thermal stabilities of aromatic hydrocarbons observed in the aqueous-pyrolysis experiments discussed preceding. Activation energies for hydrocarbon-generation reactions (from kerogen) have been experimentally estimated from both open- and closed-system pyrolysis to be in the range of 42–58 kcal/mole, varying as a function of organic-matter type or experimental method (Akihisa, 1978; Lewan, 1985; Ungerer and others, 1986; Burnham and others, 1987; Novelli and others, 1987; Tissot and others, 1987; Espitalié, Ungerer, and others, 1988; Burnham, 1989; Castelli and others, 1990). Most hydrocarbon generation (and decrease in hydrogen index) occurs in the vitrinite reflectance range of 0.8–1.6 percent (in type III organic matter, fig. 4). Thus, hydrocarbon-thermal destruction, which must overcome activation energies of 82.6–117 kcal/mole, would be expected to occur only at extreme maturation ranks, assuming that the reaction mechanics are the same as or similar to those involved with hydrocarbon generation.

In addition to the data discussed above for high-rank rocks at high burial temperatures from deep wellbores, C_{15}+ hydrocarbons have been reported by different investigators from a variety of high-temperature geologic settings. Baker and Claypool (1970) found measurable concentrations of Soxhlet-extractable hydrocarbons in various metamorphic rocks. Forsman and Hunt (1958) reported remnant hydrocarbon-generation capacity, as determined by hydrogenolysis, in some kerogens in metamorphic rocks. Hoering and Hart (1964) reported that kerogen in a graphite schist still retained remnant generation potential for both methane and heavier hydrocarbons. Shepeleva and others (1990) described aromatic hydrocarbon suites in kimberlite pipes, hydrothermal ore deposits, and crystalline bedrock in the Daldyn-Alakit region, Siberia, Russia. Goffé and Villey (1984) reported crude-oil-like hydrocarbon distributions in mineral inclusions in metamorphic rocks in the French Alps. High-temperature (300˚C–350˚C) petroleum in the hydrothermal vent water of the Guaymas Basin spreading center is well known (Simoneit, 1983, 1984, 1985; Simoneit and

others, 1984; Kawka and Simoneit, 1987; Simoneit and Kawka, 1987).

The above data allow the conclusion that not only methane but also C_{15}+ hydrocarbons are thermally stable in fine-grained rocks to much higher maturation ranks than called for by current petroleum-geochemical paradigms (fig. 1). C_{15}+ hydrocarbons apparently approach thermal destruction in the range of vitrinite reflectance=7.0–8.0 percent depending on basin variables. Methane clearly would be thermally stable to far higher temperatures and ranks than vitrinite reflectance of 7.0–8.0 percent. For example, it is well known among metamorphic petrologists that methane is thermally stable within the graphite-methane-water-carbon dioxide system to at least 800˚C (fig. 31), and it is likely that methane survives to far higher temperatures, probably extending well into the mantle (Hal Helgeson, written commun., 1991).

Lastly, it must be noted that high to moderate concentrations of C_{15}+ hydrocarbons at extreme maturation ranks (R_o=2.0–6.0 percent) and high burial temperatures (200˚C–300˚C or higher) for periods of geologic time as long as 300 million years would not be possible if organic-matter metamorphic reactions proceeded by first-order reaction kinetics. Thus, the very existence of such high-rank C_{15}+ hydrocarbons over long periods of geologic time seems to preclude the possibility that C_{15}+ hydrocarbon destruction reactions are first-order reactions.

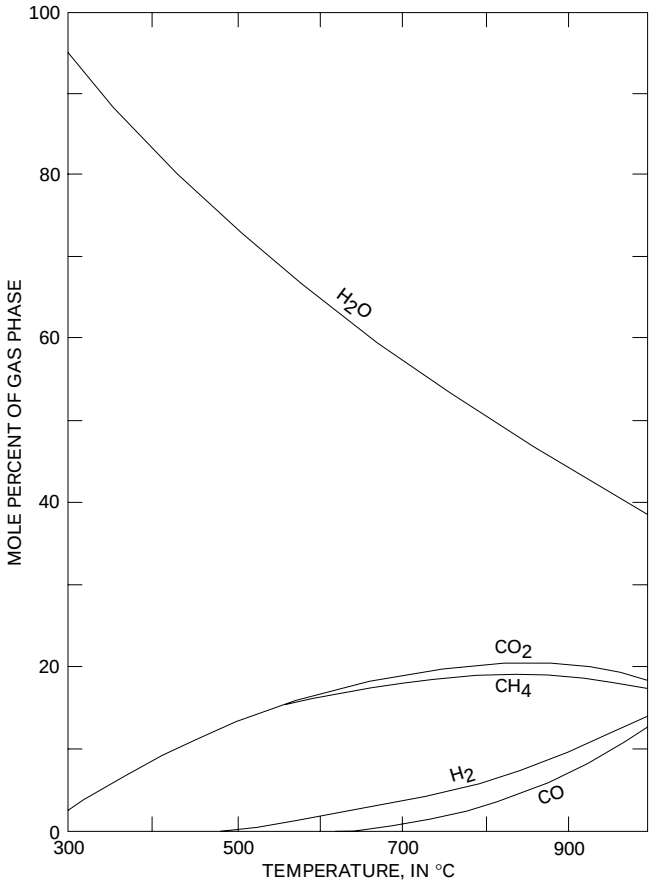

Figure 31. Phase diagram of gas species in equilibrium with graphite at a pressure of 1,000 bars. Modified from Winkler (1976).

CONCLUSIONS

1. By accepted paradigms in petroleum geochemistry, C_{15}+ hydrocarbons are destroyed by vitrinite reflectance=1.35 percent, C_2+ hydrocarbons by R_o=2.00 percent, and methane by R_o=4.00 percent. In reality, however, (a) C_{15}+ hydrocarbons are thermally stable to ranks as high as R_o=7.0–8.0 percent in deep, unsheared, petroleum basins; (b) hydrocarbon gases are thermally stable to even higher ranks, well into true rock metamorphism; and (c) methane is stable probably into mantle conditions. These hydrocarbon thermal stabilities carry no connotations, however, for the existence of conventional oil or gas deposits extending to those respective ranks, and such deposits may not necessarily be expected at those ranks.

2. C_{15}+ hydrocarbon thermal stability comes from several lines of evidence: (a) petroleum-geochemical analyses of ultradeep (7–10 km), high-rank (R_o=2.0–8.0 percent), fine-grained rocks, analyses that demonstrate that moderate to high concentrations of C_{15}+ hydrocarbons survive to these ranks; (b) compositional changes in both the saturated and aromatic hydrocarbons in the approach to and during C_{15}+ hydrocarbon-thermal destruction, changes that have been only occasionally observed in the deepest rocks of sedimentary basins; (c) long-established physical-chemical laws, which demonstrate that C_{15}+ saturated, and especially aromatic, hydrocarbons are thermally stable species with high bond energies; and (d) published data, which demonstrate that low concentrations of C_{15}+ hydrocarbons persist into conditions of true rock metamorphism and other high-temperature settings.

3. According to paradigms of present-day petroleum geochemistry, the controlling parameters of organic-matter metamorphism are burial temperature and geologic time, that is, first-order reaction kinetics. These controlling parameters predict C_{15}+ hydrocarbon-thermal destruction by R_o=1.35 percent. This prediction is in strong contrast with observed C_{15}+ hydrocarbon thermal stability to R_o=7.0–8.0 percent. Furthermore, it is maintained herein that no *solid* evidence exists that allows the conclusion that organic-matter metamorphism follows first-order reaction kinetics. Thus, it is concluded that the controlling parameters of organic-matter metamorphism, according to present-day petroleum-geochemical paradigms, must be at least partly in error.

4. Alternate controlling parameters of organic-matter metamorphism are hypothesized herein based on long-term research on the topic. Increase in burial temperature is the principal drive for the reactions, a conclusion in agreement with accepted models. Other controlling parameters and

characteristics of organic-matter metamorphic reactions are also hypothesized: (a) increases in static fluid pressures retard all aspects of organic-matter metamorphism; (b) the presence of water enriches (hydrogenates) kerogen and suppresses hydrocarbon-thermal destruction; (c) open reaction sites (product escape) promote organic-matter metamorphism, and closed reaction sites (product retention) retard organic-matter metamorphism; (d) organic-matter metamorphic reactions are not first-order reactions but instead are higher ordered reactions; and (e) reactivities of the different kerogen (organic matter) types vary, increasing with increase in sulfur content and generally decreasing with increase in hydrogen content. Thus, type II–S organic matter reacts before type III organic matter, which reacts before type II organic matter, which reacts before type I organic matter.

REFERENCES CITED

Akihisa, K., 1978, Etude cinétique des roches mères de pétrole (rapport n 4)—Formation de produits pétroliers par pyrollyse du kérogene à basse température: Journal Japanese Association Petroleum Technology, v. 44, p. 26–33.

Baker, D.R., and Claypool, G.E., 1970, Effects of incipient metamorphism on organic matter in mudrock: American Association of Petroleum Geologists Bulletin, v. 54, p. 456–468.

Barker, C., and Takach, N.E., 1992, Prediction of natural gas composition in ultradeep sandstone reservoirs: American Association of Petroleum Geologists Bulletin, v. 76, p. 1859–1873.

Barker, C.E., 1991, Implications for organic maturation studies of evidence for a geologically rapid increase and stabilization of vitrinite reflectance at peak temperature—Cerro Prieto geothermal system, Mexico: American Association of Petroleum Geologists Bulletin, v. 75, p. 1852–1863.

Bertrand, P., 1984, Geochemical and petrographic characterization of humic coals considered as possible source rocks: Organic Geochemistry, v. 6, p. 481–488.

Bostick, N., 1970, Thermal alteration of clastic organic particles (phytoclasts) as an indicator of contact and burial metamorphism in sedimentary rocks: Palo Alto, Calif., Stanford University Ph. D. thesis.

Braun, R.L., and Burnham, A.K., 1990, Mathematical model of oil generation, degradation, and expulsion: Energy and Fuels, v. 4, p. 132–146.

Brooks, T.D., 1971, Some chemical and geochemical studies on sporopollenin, *in* Brooks, J., Grant, P.R., Muir, M., Gijzel, P., and Shaw, G., eds., Sporopollenin: London, Academic Press, p. 351–407.

Burnham, A.K., 1989, A simple model of petroleum formation and cracking: Lawrence Livermore Laboratory Report UCID 21665, March 1989.

Burnham, A.K., Braun, R.L., and Gregg, H.R., 1987, Comparison of methods for measuring kerogen pyrolysis rates and fitting kinetic parameters: Journal of Energy Fuels, v. 1, p. 452–458.

Castelli, A., Chiaramonte, M. A., Bettrame, P.L., Carniti, P., Delbianco, A., and Stroppa, F., 1990, Thermal degradation of kerogen by hydrous pyrolysis—A kinetic study: Organic Geochemistry, v. 16, p. 75–82.

Cecil, B., Stanton, R., Allshouse, S., and Cohen, M.A., 1979, Effects of pressure on coalification: International Congress of Carboniferous Stratigraphy and Geology, 9th, Urbana, Illinois, May 19–26, Abstracts of Papers, p. 32.

Chung, M., and Sackett, W., 1978, Carbon isotope fractionation during coal pyrolysis: Fuel, v. 57, p. 734–735.

Connan, J., 1974, Time-temperature relation in oil genesis: American Association of Petroleum Geologists Bulletin, v. 58, p. 2516–2521.

Connan, J., Montel, F., Blanc, P.H., Sahuquet, B., and Jouhannel, R., 1991, Experimental study of expulsion of hydrocarbons from shaley source rocks—Importance of pressure on expulsion efficiencies, *in* Manning, D.A.C., ed., Advances in organic geochemistry: Advances and Applications in Energy and the Natural Environment, Program and Abstracts, p. 14–15.

Cooles, G.P., Mackenzie, A.S., and Quigley, T.M., 1986, Calculation of petroleum masses generated and expelled from source rocks: Organic Geochemistry, v. 10, p. 235–245.

Cottrell, T.L., 1958, The strengths of chemical bonds: Butterworths.

Domine, F., 1991, High pressure pyrolysis of n-hexane, 2-4 dimethylpentane and 1-phenylbutane—Is pressure an important geochemical parameter?: Organic Geochemistry, v. 17, p. 619–634.

Domine, F., and Enguehard, F., 1992, Kinetics of hexane pyrolysis at very high pressures—Application to geochemical modeling: Organic Geochemistry, v.18, p. 41–49.

Eggers, D.F., Gregory, N.W., Halsey, G.D., and Rabinovitch, B.S., 1964, Physical chemistry: London, Wiley and Sons, 783 p.

Espitalié, J., Maxwell, J. R., Chenet, Y., and Marquis, F., 1988, Aspects of hydrocarbon migration in the Mesozoic in the Paris Basin as deduced from an organic geochemical survey: Organic Geochemistry, v. 13, p. 457–481.

Espitalié, J., Ungerer, P., Irwin, I., and Marquis, F., 1988, Primary cracking of kerogens—Experimenting and modeling C_1, C_2-C_5, C_1-C_{15} and C_{15}+ classes of hydrocarbons formed: Organic Geochemistry, v. 13, p. 893–899.

Forsman, J.P., and Hunt, J.M., 1958, Insoluble organic matter (kerogen) in sedimentary rock of marine origin, *in* Weeks, L.G., ed., Habitat of oil: American Association of Petroleum Geologists, p. 747–778.

Goffé, B., and Villey, M., 1984, Texture d'un matériel carboné impliqué dans un metamorphisme haute pression-basse température (Alpes Francaises)—Les hautes pressions influenant, elles la carbonification?: Bulletin de Mineralogie, v. 107, p. 81–91.

Goodarzi, F., and Murchison, D., 1977, Effect of prolonged heating on the optical properties of vitrinite: Fuel, v. 56, p. 89–96.

Gould, E.S., 1959, Mechanism and structure in organic chemistry: Henry Holt and Co.

Hayes, J.M., 1991, Stability of petroleum: Nature, v. 352, July 11, p. 108–109.

Helgeson, H., 1991, Organic/inorganic reactions in metamorphic processes: Canadian Mineralogist Greenwood Symposium Issue, v. 29, p. 707–739.

Hesp, W., and Rigby, D., 1973, The geochemical alteration of hydrocarbons in the presence of water: Erdöl und Kohle-Erdgas, v. 26, p. 70–76.

Hoering, T.C., and Abelson, P.H., 1964, Hydrocarbons from the low-temperature heating of a kerogen: Carnegie Institute Yearbook 1963–1964, v. 1440, p. 256–258.

Hoering, T.C., and Hart, R., 1964, A geochemical study of some Adirondack graphites: Carnegie Institute Yearbook 1963–1964, v. 1440, p. 265–267.

Hunt, J.M., 1979, Petroleum geochemistry and geology: San Francisco, Freeman and Company, 617 p.

Ishiwatari, R., Ishiwatari, M., Rohrback, B.G., and Kaplan, I.R., 1977, Thermal alteration experiments on organic matter from recent marine sediments in relation to petroleum genesis: Geochimica et Cosmochimica Acta, v. 41, p. 815–828.

Karweil, J., 1956, Die metamorphose der kohlen vom standpunkt der physikalische chemie: Zeitschrift Deutsche Geologishe Gesellschaft, v. 107, p. 132–139.

Kawka, O.E., and Simoneit, B.R.T., 1987, Survey of hydrothermally-generated petroleums from the Guaymas Basin spreading center: Organic Geochemistry, v. 11, p. 311–328.

Klotz, I.M., 1964, Introduction to chemical thermodynamics: New York, W.A. Benjamin, 244 p.

Kontorovich, A.E., and Trofimuk, A.A., 1976, Lithogenezi neftegazoobrazoveniye (Lithogenesis and formation of oil and gas), *in* Vassoyevich, N.B., and others, eds., Goryuchiye Iskopayeme-Problemy Geoloii i Geokhiii Noftidov i Bituminoznykh Porod, Mezhdunarodnyy Geologicheskiy Kongress XXV Sessiya Doklady Sovetskikh Geologov: Moscow, Nauka Press, p. 19–36.

Lewan, M.D., 1983, Effects of thermal maturation on stable organic carbon isotopes as determined by hydrous pyrolysis of Woodford Shale: Geochimica et Cosmochimica Acta, v. 47, p. 1471–1479.

———1985, Evaluation of petroleum generation by hydrous pyrolysis experimentation: Philosophical Transactions of the Royal Society of London, v. 315, p. 123–134.

———1993, Laboratory simulation of petroleum formation—Hydrous pyrolysis, *in* Engel, M.H., and Macko, S.A., eds., Organic geochemistry: New York, Plenum Press, p. 419–442.

Leythaeuser, D., Littke, R., Radke, M., and Schaefer, R.G., 1988, Geochemical effects of petroleum migration and expulsion from Toarcian source rocks in the Hills syncline area, NW Germany: Organic Geochemistry, v 13, p. 489–502.

Leythaeuser, D., Miller, P.J., Radke, M., and Schaefer, R.G., 1987, Geochemistry can trace primary migration of petroleum—Recognition and quantification of expulsion effects, *in* Doligez, B., ed., Migration of hydrocarbons in sedimentary basins: Paris, Editions Technip, p. 197–222.

Lopatin, N.V., 1971, Temperature and geologic time as factors in coalification: Akademiya Nauk SSSR Serial Geologicheskaya, Izvestiya 3, p. 95–106. (Translation by N.H. Bostick.)

Mackenzie, A.S., Price, I., Leythaeuser, D., Muller, P., Radke, M., and Schaefer, R.G., 1987, The expulsion of petroleum from Kimmeridge clay source rocks in the area of the Brae Oilfield, UK Continental Shelf, *in* Brooks, J., and Glennie, K., eds., Petroleum geology of northwest Europe: Graham and Trotman, p. 865–877.

Mango, F.D., 1990, The origin of light cycloalkanes in petroleum: Geochimica et Cosmochimica Acta, v. 54, p. 23–27.

Mango, F., 1991, The stability of hydrocarbons under time-temperature conditions of petroleum genesis: Nature, v. 352, p. 146–148.

McIntyre, D.J., 1972, Effect of experimental metamorphism on pollen in a lignite: Geoscience and Man, v. 4, p. 111–117.

McTavish, R.A., 1978, Pressure retardation of vitrinite diagenesis, offshore northwest Europe: Nature, v. 271, p. 648–650.

Monthioux, M., Landais, P., and Durand, B., 1986, Comparison between extracts from natural and artificial maturation series of Mahakam delta coals: Organic Geochemistry, v. 10, p. 299–311.

Novelli, L., Chiaramonte, M.A., Mattavelli, L., Pizzi, G., Satori, L., and Scotti, P., 1987, Oil habitat in the Northwestern Po Basin, *in* Doligez, B., ed., Migration of hydrocarbons in sedimentary basins: Paris, Editions Technip, p. 27–58.

Orr, W.L., 1986, Kerogen/asphaltene/sulfur relationships in sulfur-rich Monterey oils: Organic Geochemistry, v. 10, p. 499–516.

Pauling, L., 1960, The nature of the chemical bond: Ithaca, New York, Cornell University Press.

Pearson, D.B., 1981, Experimental simulation of thermal maturation in sedimentary organic matter: Houston, Texas, Rice University Ph. D. thesis.

Phillipi, G.T., 1965, On the depth, time, and mechanism of petroleum generation: Geochimica et Cosmochimica Acta, v. 29, p. 1021–1051.

Price, L.C., 1982, Organic geochemistry of 300˚C, 7-km core samples, South Texas: Chemical Geology, v. 37, p. 205–214.

———1983, Geologic time as a parameter in organic metamorphism and vitrinite reflectance as an absolute paleogeothermometer: Journal of Petroleum Geology, v. 6, p. 5–38.

———1985, Geologic time as a parameter in organic metamorphism and vitrinite reflectance as an absolute paleogeothermometer—Reply: Journal of Petroleum Geology, v. 8, p. 233–240.

———1988, The organic geochemistry (and causes thereof) of high-rank rocks from the Ralph Lowe–1 and other wellbores: U.S. Geological Survey Open-File Report 91–307, 55 p.

———1989a, Primary petroleum migration from shales with oxygen-rich organic matter: Journal of Petroleum Geology, v. 12, p. 289–324.

———1989b, Hydrocarbon generation and migration from type III kerogen as related to the oil window: U.S. Geological Survey Open-File Report 89–194.

———1991, Considerations of oil origin, migration, and accumulation at Caillou Island and elsewhere in the Gulf Coast: U.S. Geological Survey Open-File Report 91–307, 55 p.

———1994, Basin richness versus source rock disruption from faulting—A fundamental relationship?: Journal of Petroleum Geology, v. 17, p. 5–38.

Price, L.C., and Barker, C.E., 1985, Suppression of vitrinite reflectance in amorphous rich kerogen—A major unrecognized problem: Journal of Petroleum Geology, v. 8, p. 59–84.

Price, L.C. and Clayton, J.L., 1990, Reasons for and significance of deep, high-rank hydrocarbon generation in the South Texas Gulf Coast, *in* Schumacher, D., and Perkins, B.F., eds., Gulf Coast oils and gases: Annual Research Conference, Gulf Coast Section, Society of Economic Paleontologists and Mineralogists, 9th, Proceedings, 105–137.

———1992, Extraction of whole versus ground source rocks—Fundamental petroleum geochemical implications

including oil-source rock correlation: Geochimica et Cosmochimica Acta, v. 56, p. 1213–1222.

Price, L.C., Clayton, J.L., and Rumen, L.L., 1979, Organic geochemistry of a 6.90 kilometer-deep well, Hinds County, Mississippi: Transactions Gulf Coast Geological Society, v. 29, p. 352–370.

———1981, Organic geochemistry of the 9.6 km Bertha Rogers #1, Oklahoma: Journal of Organic Geochemistry, v. 3, p. 59–77.

Price, L.C., Ging, T.G., Daws, T.A., Love, A.H., Pawlewicz, M.J., and Anders, D.E., 1984, Organic metamorphism in the Mississippian-Devonian Bakken shale North Dakota portion of the Williston Basin, *in* Woodward, J., Meissner, F.F., and Clayton, J.L., eds., Hydrocarbon source rocks of the greater Rocky Mountain Region: Denver, Rocky Mountain Association of Geologists, p. 83–113.

Price, L.C., and Le Fever, J.A., 1992, Does Bakken horizontal drilling imply huge oil-resource bases in fractured shales?, *in* Schmoker, J., ed., Geological studies relevant to horizontal drilling, examples from Western North America: Rocky Mountain Association of Geologists, p. 199–214.

Price, L.C., and Wenger, L.M., 1991, The influence of pressure on petroleum generation and maturation as suggested by aqueous pyrolysis: Organic Geochemistry, v. 19, p. 141–159.

Quigley, T.M., and Mackenzie, A.S., 1988, The temperatures of oil and gas formation in the sub-surface: Nature, v. 333, p. 549–552.

Roberts, J.D., and Caserio, M.C., 1964, Basic principles of organic chemistry: Amsterdam, W.A. Benjamin, 1315 p.

Rogers, J., Suggate, R., Elphick, J., and Ross, J., 1962, Metamorphism of a lignite: Nature, v. 195, p. 1078–1080.

Sagjo, Cs., 1980, Hydrocarbon generation in a super-thick Neogene sequence in south-east Hungary—A study of the extractable organic matter, *in* Douglas, A.G., and Maxwell, A.G., eds., Advances in organic geochemistry 1979: Great Britain, Pergamon, p. 103–113.

Sassen, R., and Moore, C.H., 1988, Framework of hydrocarbon generation and destruction in eastern Smackover trend: American Association of Petroleum Geologists Bulletin, v. 72, p. 649–663.

Shock, E., 1990, Geochemical considerations of the origin of organic compounds in hydrothermal systems: Origins of Life and Evolution of the Biosphere, v. 20, p. 331–367.

Shepeleva, N.N., Ogloblina, A.I., and Pikovskiy, Yu I., 1990, Polycyclic aromatic hydrocarbons in carbonaceous material from the Daldyn-Alakit region, Siberian Platform: Geochemistry International, v. 28, 4, p. 98–107.

Sienko, M.J., and Plane, R.A., 1961, Chemistry: Toronto, Ont., McGraw-Hill, 623 p.

Simoneit, B.R.T., 1983, Organic-matter maturation and petroleum genesis—Geothermal versus hydrothermal, *in* The role of heat in the development of energy and mineral resources in the Northern Basin and Range Province: Davis, Calif., Geothermal Resources Council, Special Report 13, p. 215–241.

———1984, Hydrothermal effects on organic matter—High versus low temperature components: Organic Geochemistry, v. 6, p. 857–864.

———1985, Hydrothermal petroleum—Genesis, migration and deposition in Guaymas Basin, Gulf of California: Canadian Journal of Earth Sciences, v. 22, p. 1919–1929.

Simoneit, B.R.T. and Kawka, O.E., 1987, Hydrothermal petroleum from diatomites in the Gulf of California, *in* Brooks, J., and Fleet, A., eds., Marine petroleum source rock: Geological Society of London Special Publication 26, p. 217–228.

Simoneit, B.R.T., Philp, R.P., Jenden, P.D., and Galimov, E.M., 1984, Organic geochemistry of Deep Sea Drilling Project sediments from the Gulf of California—Hydrothermal effects on unconsolidated diatomooze: Organic Geochemistry, v. 7, p. 173–205.

Sokolov, V.A., Geodekyan, A.A., Grigoryev, C.G., Krems, A.Ya., Stroganov, V. A., Zorkin, L.M., Zeidelson, M.I., and Vainbaum, S. Ja., 1971, The new methods of gas surveys, gas investigations of wells and some practical results, *in* Boyle, R.W., ed., Geochemical exploration: Canadian Institute of Mining and Metallurgy Special Volume 11, p. 538–544.

Takach, N.E., Barker, C., and Kemp, M.K., 1987, Stability of natural gas in the deep subsurface—Thermo-dynamic calculation of equilibrium compositions: American Association of Petroleum Geologists Bulletin, v. 71, p. 322–333.

Talukdar, S., Gallango, O., Vallejos, C., and Ruggiero, A., 1987, Observations on the primary migration of La Luna source rocks of the Maracaibo Basin, Venezuela, *in* Doligez, B., ed., Migration of hydrocarbons in sedimentary basins: Paris, Editions Technip, p. 59–77.

Teichmüller, M., and Durand, B., 1983, Fluorescence microscopial rank studies on liptinites and vitrinites in peats and coals and comparison with results of the Rock-Eval pyrolysis: International Journal of Coal Geology, v. 2, p. 197–230.

Tissot, B.P., Pelet, R., and Ungerer, P.H., 1987, Thermal history of sedimentary basins, maturation indices, and kinetics of oil and gas generation: American Association of Petroleum Geologists Bulletin, v. 71, p. 1445–1466.

Tissot, B.P., and Welte, D.H., 1984, Petroleum formation and occurrence: Berlin, Springer Verlag, 699 p..

Ungerer, P., 1990, State of the art research in kinetic modeling of oil formation and expulsion: Organic Geochemistry, v. 16, p. 1–25.

Ungerer, P., Chenet, P.Y., Moretti, I., Chiarelli, A., and Oudin, J.L., 1986, Modeling oil formation and migration in the southern part of the Suez rift, Egypt: Organic Geochemistry, v. 10, p. 247–260.

Ungerer, P., Doligez, B., Chenet, P.Y., Burrus, J., Bessis, F., Lefargue, E., Giroir, G., Heurn, O., and Eggen, S., 1987, A 2-D model of basin scale petroleum migration by two-phase fluid flow application to some case studies, *in* Doligez, B., ed., Migration of hydrocarbons in sedimentary basins: Paris, Editions Technip, p. 415–456.

Wenger, L.M., and Price, L.C., 1991, Differential petroleum generation and maturation paths of the different organic matter types as determined by hydrous pyrolysis over a wide range of experimental temperatures, *in* Manning, D.A.C., ed., Advances in organic geochemistry: Advances and Applications in Energy and the Natural Environment, Program and Abstracts, p. 335–339.

Winkler, H.G.F., 1976, Petrogenesis of metamorphic rocks: New York, Springer Verlag, 334 p.

Zumberge, J.E., Sutton, C., Martin, S.J., and Worden, R.D., 1988, Determining oil generation kinetic parameters by using a fused quartz pyrolysis system: Energy and Fuels, v. 2, p. 264–266.